J. Physiol. (1980), **306**, *pp.* 377–410
With 21 text-figures
Printed in Great Britain

VOLTAGE-CLAMP EXPERIMENTS IN NORMAL AND DENERVATED MAMMALIAN SKELETAL MUSCLE FIBRES

BY PAMELA A. PAPPONE*

From the Department of Physiology and Biophysics, SJ-40, University of Washington, Seattle, Washington 98195, U.S.A.

(*Received 9 January 1979*)

SUMMARY

1. The vaseline-gap voltage-clamp method has been applied to the study of ionic currents in cut pieces from innervated and 5–7 day denervated rat skeletal muscle fibres.

2. Kinetic analysis of sodium currents in innervated rat muscle showed them to be similar to those in frog muscle, except that rat sodium channels are activated at slightly more negative potentials. Peak sodium conductances of 40–50 m-mho/cm^2 were measured, corresponding to values of $\bar{G}_{Na}$ of 100–120 m-mho/cm^2.

3. The permeability sequence of the sodium channel to several organic and inorganic cations is $Li^+ > Na^+ >$ hydroxylammonium $>$ hydrazinium $>$ guanidinium $\approx$ ammonium $> K^+$. TMA^+ and Ca^{2+} were not measurably permeant.

4. Denervation appears to shift activation and inactivation parameters of sodium currents by ~ 10 mV to more negative potentials, but does not appreciably affect the maximum peak sodium conductance or the time constants for activation and inactivation.

5. Dose–response curves for block by tetrodotoxin in innervated fibres are fitted well by assuming binding of toxin to a single population of channels with a dissociation constant of about 5 nM. In denervated fibres there appears in addition a second population of channels with a dissociation constant in the micromolar range. These relatively toxin-insensitive channels respond less rapidly to potential changes, and can contribute up to 25–30 % of the total sodium conductance.

6. The potassium currents of innervated rat muscle were similar to those of frog muscle in their voltage dependence of activation.

7. The time constant for inactivation of the sodium current, τ_h, at -13 mV showed a temperature dependence measured between 10 and 20 °C equivalent to an average Q_{10} of 2·3. The Q_{10} for the time constant of activation of the potassium current, τ_n, averaged 2·5 between -40 mV and $+40$ mV, measured over the same temperature range.

* Present address: Department of Physiology, University of California, Irvine, California 92717, U.S.A.

0022-3751/80/1640–0950 $07.50

INTRODUCTION

Voltage-clamp studies of frog skeletal muscle have contributed greatly to our understanding of membrane excitation in that tissue (Adrian, Chandler & Hodgkin, 1970; Idelfonse & Roy, 1972; Adrian & Peachey, 1973; Campbell & Hille, 1976). The membrane events underlying action potential generation in mammalian skeletal muscle have not been as well characterized. Such information is necessary for the understanding of excitation in normal mammalian muscle and to ascertain the changes responsible for the altered excitability occurring, for example, in myotonic muscle or following denervation.

Recent experiments have shown that the membrane currents of mammalian muscle under voltage clamp are qualitatively similar to those of frog muscle (Pappone, 1977; Adrian & Marshall, 1977; Duval & Leóty, 1978). This paper presents a full account of the conductance changes during depolarization in cut pieces from fast-twitch rat skeletal muscle fibres studied using the vaseline-gap clamp. I have also investigated the effects of denervation on the sodium currents. Activation and inactivation of sodium current occurred at more negative potentials in denervated fibres. In addition, following denervation a new type of sodium channel is present in the membrane. The new channel differs from the normal sodium channel in its kinetics and sensitivity to tetrodotoxin. It is this new sodium channel which is probably responsible for the tetrodotoxin-resistant action potentials of denervated mammalian muscle (Harris & Thesleff, 1971; Redfern & Thesleff, 1971b).

METHODS

Preparation. Voltage-clamp experiments were performed on single muscle fibres from the rat. Large animals (400–800 g) were used because the single fibre dissection was easier in these than in smaller rats. The animals were killed by a blow to the head, and the isolated muscle was pinned in a dissecting dish. The muscle was continuously perfused with oxygenated Tyrode's solution (composition: 135 mM-NaCl, 5 mM-KCl, 2 mM-$CaCl_2$, 1 mM-$MgCl_2$, 12 mM-NaH_2CO_3, 1 mM-Na_2HPO_4, 11 mM-glucose, bubbled with 95% O_2+5% CO_2) at room temperature. Fibres in good condition could be obtained from muscles kept under these conditions for up to 9 h.

Results for fibres from three rat muscles are reported here: the white part of the innervated sternomastoid (s.m.), innervated extensor digitorum longus (e.d.l.), and chronically denervated e.d.l. Both e.d.l. and the white part of s.m. contain predominantly fast-twitch type fibres. E.d.l. fibres were denervated by cutting out a ~1 cm piece of the peroneal nerve above the knee with the animal under ether anaesthesia. Experiments were performed on the denervated muscles 5–7 days following the surgery.

A 6–8 mm piece of a single fibre was dissected from the muscle and mounted in the experimental chamber in a 160 mM-CsF or K glutamate solution as described by Hille & Campbell (1976). Fibres contracted during this procedure and the average fibre diameter increased from 50–70 μm before dissection to about 90 μm. A diagram of the preparation in the experimental chamber is shown in Fig. 1, with usual dimensions indicated. After fibre and vaseline seals were in place, the solution in the A pool was changed to Ringer, and in some experiments the solutions in the C and the E pools were exchanged for EGTA-containing solutions.

Voltage clamp. The voltage-clamp system used here is the vaseline-gap method developed for frog muscle fibres by Hille & Campbell (1976) and modified by Schwarz, Palade & Hille (1977). It is based on the method used by Frankenhaeuser (1957) and Dodge and Frankenhaeuser (1958) for studies of myelinated nerve. An outline of the voltage-clamp circuit is shown in Fig. 1. The length of the fibre in the A pool was typically 100 μm.

The membrane current was measured from the voltage drop across a 10 kΩ resistor in series with the E pool. This measure of the membrane current will be in error if a significant portion of the current injected at E flows through the EA seal rather than through the fibre membrane. The seal resistance, R_{EA}, can be measured by eliciting an action potential with a short stimulating current with the fibre under current clamp. Following the stimulus, the E pool is held at ground and all the current seen is through the EA seal. The current during an action potential of 140 mV amplitude was less than 20 nA in four typical preparations, corresponding to an R_{EA} of at least 7 MΩ. The average value of the parallel combination of R_{EA} and the resistance

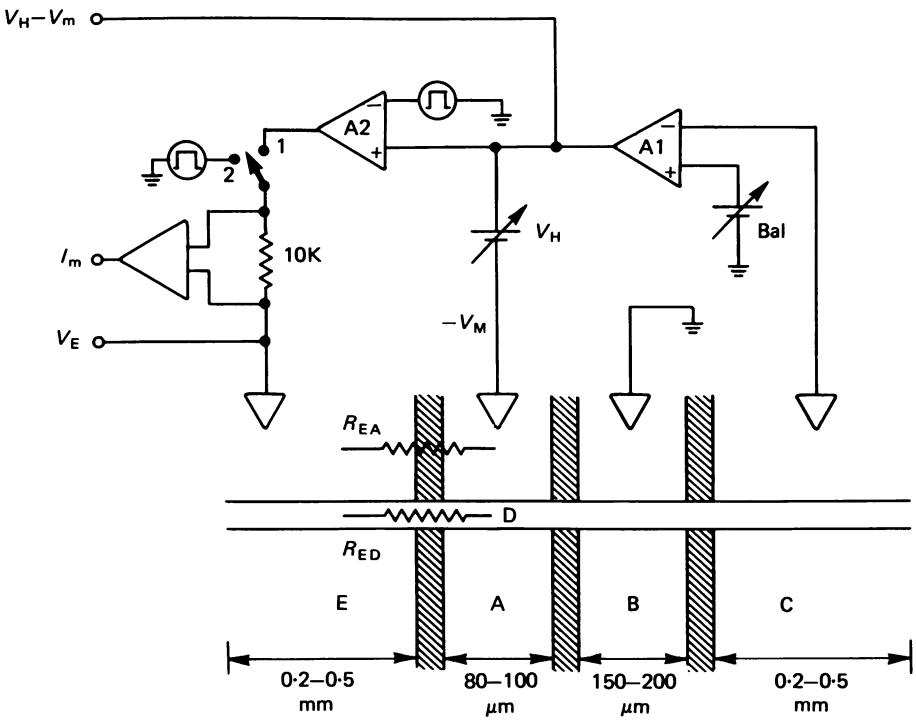

Fig. 1. Schematic drawing of the fibre in the experimental chamber and the voltage-clamp circuit. A, B, C and E are solution-filled pools in the chamber connected by calomel electrodes to the voltage-clamp circuit. Typical dimensions of the length of fibre in pools A and B are indicated, as are the lengths of the fibre ends in pools C and E. Vaseline seal dimensions were BC = 500 μm, AB = 200 μm, EA = 200 μm. R_{EA} is the resistance of the seal between E and A pools. Point D is the interior of the fibre in the A pool, and R_{ED} the resistance between the E pool and point D through the cut end of the fibre. The values of $V_H - V_m$, the holding potential minus the membrane potential, the current (I_m) through the E pool, and the voltage in the E pool (V_E) were externally available for measurement. With the switch in position 1, the circuit is in voltage-clamp mode, and in position 2 in current clamp mode.

through the fibre was 140 kΩ, measured from the voltage in, and current through, the E pool ($R_{EA} = V_E/I_m$). Thus, the average resistance of the current path E→D was 143 kΩ, and more than 98% of any current injected into the E pool flowed through the fibre membrane in the A pool.

The potentiometric method of voltage clamping depends on the inside of the fibre, point D, being held at ground by the amplifier A1. For this to be accomplished, A1 must have enough gain to control deviations of point D from ground, and A1 must be correctly balanced. These points can be tested by recording the potential at point D with a micro-electrode. Fig. 2 shows an action potential recorded in the vaseline gap in current clamp mode. The amplitude of the

action potential is 143 mV. The lower trace shows the potential inside the fibre, V_D, recorded with a micro-electrode. The maximum deviation of V_D from ground occurs during the rising phase of the action potential and is only 0·5 mV. Thus, the characteristics of the circuit are adequate to control the internal potential when there is no net current flow. Even when a depolarizing voltage step elicited a sodium current of peak amplitude 0·55 μA in this fibre, the deviation from ground was <1 mV. Small deviations of 1·5 mV were seen at the onset and

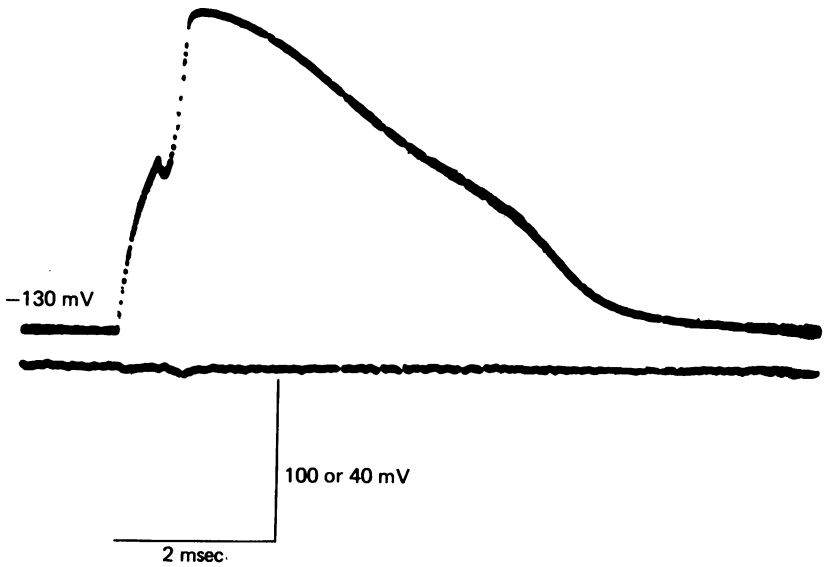

Fig. 2. Top trace: action potential in the vaseline gap in an innervated s.m. fibre at 12 °C, 100 mV voltage scale. Lower trace: V_D recorded simultaneously with a micro-electrode, 40 mV scale. Voltage is inverted relative to the upper trace. Fibre 9/28/1. Ends cut in CsF.

offset of the voltage step, indicating that the high-frequency potential changes were less well controlled. With a more typical peak sodium current of 2 μA, the expected deviation in V_D would still be <4 mV. The expected longitudinal voltage non-uniformity can be calculated from cable theory (Hille & Campbell, 1976, eqn (3)) to average 3 mV for the maximum sodium currents.

Correct balancing of A1 is crucial for measurement of absolute membrane potential by this method. Two methods of balancing were used in the present experiments. Neither proved consistently satisfactory, and for the precise measurement of membrane potential it would probably be better to use a micro-electrode measurement of V_D to balance A1. The first method, which will be termed the zero method, is the same as used by Hille & Campbell (1976). With no current injected into the E pool, one assumes that the potential of the membrane in the A pool is -90 mV. The negative of this value is set on the variable battery 'V_H' in Fig. 1, and then the battery 'Bal' is adjusted until the output of A1 reads zero. With this method, V_D measured with a micro-electrode is slightly positive; six fibres gave an average value of $+1{\cdot}3$ mV $\pm$ 0·11 mV (S.E. of mean), and the absolute measurement for V_m would be too positive by the same amount. In the second method, termed the B – C method, pools B and C are made to coalesce, establishing electrical connection between B and C electrodes, the output of A1 is disconnected from the A pool and 'Bal' is adjusted until the output of A1 is at ground. This method in theory should correctly balance out potentials on the B and C electrodes, but in practice it resulted in a V_D of $-6{\cdot}1 \pm 1{\cdot}4$ mV ($n=6$). Thus, the membrane potential is slightly too negative. Either balancing procedure could result in deviations of V_D of as much as 10 mV. The method which gave the most accurate balance varied among fibres.

Compensation for series resistance was set by adjusting the appropriate circuit elements until high-frequency ringing just appeared at the onset of a voltage-clamp step. The series resistance of the chamber was adequately compensated by this procedure, since in normal fibres reducing the current to 10 % of its original amplitude by application of tetrodotoxin (TTX) resulted in no change in the time-to-peak, rate of inactivation, or voltage dependence of peak activation of the sodium current. For study of ionic currents the linear currents due to passive properties of the membrane were electronically subtracted from the current record. The parameters of the subtraction circuit were set to null the current seen during small depolarizing or hyperpolarizing voltage steps.

Temperature was controlled by means of Peltier devices in the base of the brass block containing the experimental chamber. A feed-back circuit controlling the Peltier elements used the temperature from a thermistor in or above the A pool as its input. The system was capable of changing the A pool temperature 10 °C in 5 min. In experiments examining the effects of temperature on sodium currents V_D was measured with a micro-electrode and used to balance A1.

Solutions. The solutions termed 'internal solutions' were used in the B, C, and E pools of the experimental chamber. The internal solution was allowed to diffuse into the fibre through the cut ends in the C and E pools. The experiments reported here used either 160 mM-CsF or 128 mM-K glutamate + 21·2 mM-K_2EGTA as the internal solution. Cell membrane depolarization under voltage clamp was accompanied by contraction when the internal solution was pure isotonic K_2SO_4 or K glutamate, but not when it contained fluoride or EGTA.

'External solutions' were used in the A pool surrounding the voltage clamped region of the fibre. The normal Ringer solution used for most experiments contained 135 mM-NaCl, 5 mM-KCl, 2 mM-$CaCl_2$, 1 mM-$MgCl_2$, and 15 mM-TMA-MOPS.

RESULTS

Passive electrical properties. The membrane resistance, R_m, and the effective membrane capacitance, C_{eff}, of normal and denervated muscle fibres were measured under voltage clamp. Their values are summarized in Table 1. The measurements were made from the current following a hyperpolarizing potential step of magnitude ΔV_m (Fig. 3). The final level of the current, I_{ss}, was used to calculate R_m from

$$R_m = \Delta V_m / I_{ss} \pi d l, \tag{1}$$

where d is the apparent fibre diameter and l is the length of the fibre in the A pool.

The integral of the transient portion of the current record was used to evaluate the effective membrane capacity, C_{eff} (Adrian & Almers, 1974). As expected from morphology, the current transient in response to a step change in potential showed rapid and slow phases. The fast component of the charge movement probably corresponds to the charging of the surface membrane capacitance, and the slow component to the charging of the transverse tubular system membrane through the series resistance of the tubular lumen. For an approximate separation of the two components, the current record at times longer than 0·5 msec following the potential change was fitted with an exponential function with time constant τ_s and initial amplitude I_s (0). This function was then used to calculate a slowly charging portion of the specific effective capacitance, C_s:

$$C_s = \frac{I_s(0)\,\tau_s}{\Delta V_m \pi\, dl}. \tag{2}$$

The slow component was then subtracted from the current record. The remaining fast charge movement was evaluated by integration with a planimeter and divided

by ΔV_m to obtain the rapidly charging component of the specific effective capacitance, C_f.

The values of τ_s, C_s, C_f and C_{eff}, the total effective capacitance are shown in Table 1. There is no large difference in these parameters between innervated and denervated muscles. My data scatter too much to show the small (20 %) increase in R_m reported by Albuquerque & Thesleff (1968) and Albuquerque and McIssac (1970)

TABLE 1. Passive properties

Innervated muscle fibre	d (μm)	R_m (Ω cm^2)	τ_s (msec)	C_s (μF/cm^2)	C_f (μF/cm^2)	C_{eff} (μF/cm^2)
9:27:3	80	352	1·56	3·32	1·42	4·74
1:3:3	110	498	1·08	6·38	1·84	8·22
1:5:4	110	821	1·70	8·74	2·56	11·3
4:22:1	80	628	2·59	7·11	1·49	8·60
4:22:2	90	471	3·04	8·22	1·36	9·58
4:22:3	90	389	3·10	9·98	2·80	12·8
Average	93·3	527	2·18	7·29	1·91	9·20
S.E. of mean	5·6	70·5	0·35	0·95	0·25	1·20
Denervated muscle fibre						
1:17:5	90	904	1·53	10·8	3·51	14·3
1:17:4	100	201	2·85	12·2	3·62	15·8
1:17:3	90	385	3·12	11·6	2·16	13·8
1:17:2	100	402	1·86	3·71	1·49	5·20
1:12:1	90	494	2·01	2·46	1·05	3·51
1:12:2	100	408	1·66	7·00	2·22	9·22
1:12:3	90	244	2·54	7·86	2·08	9·94
Average	94·3	434	2·22	7·95	2·30	10·3
S.E. of mean	2·0	87	0·23	1·45	0·35	1·79

in 5–7 day denervated muscles. If C_f represents the sarcolemma and C_s the transverse tubules, then the results in Table 1 would indicate that there is four times as much tubular as surface membrane per unit volume of fibre. This value is in fair agreement with the results on the ultrastructure of fast twitch mammalian muscle (Eisenberg & Kuda, 1975; Luff & Atwood, 1971), where a unit fibre volume was found to contain three times more tubular than surface membrane.

The values of membrane resistance presented here are in the lower part of the range previously reported, and the values of membrane capacitance higher than others have found. These differences are not due to leakage current through the vaseline seal between the E and A pools (see Methods). A probable explanation is that the fibres in these experiments are contracted. In frog muscle, the passive membrane properties referred to the cylindrical surface area of the fibre are dependent on the muscle length (Valdiosera, Clausen & Eisenberg, 1974; Dulhunty & Franzini-Armstrong, 1977). If the fibre contracts at constant volume, then the membrane area per unit volume of the fibre will remain constant. The total amount of membrane per unit cylinder surface will then increase approximately linearly with

fibre radius. If one assumes that the uncontracted diameter averaged 60 μm, then when contracted to an average diameter of 94 μm these fibres would be expected to have 1·57 times as much membrane area per unit cylinder surface as uncontracted fibres. If sarcolemma and tubular membranes contribute to conductance and capacity in proportion to their areas (Hodgkin & Nakajima, 1972), we would expect a specific

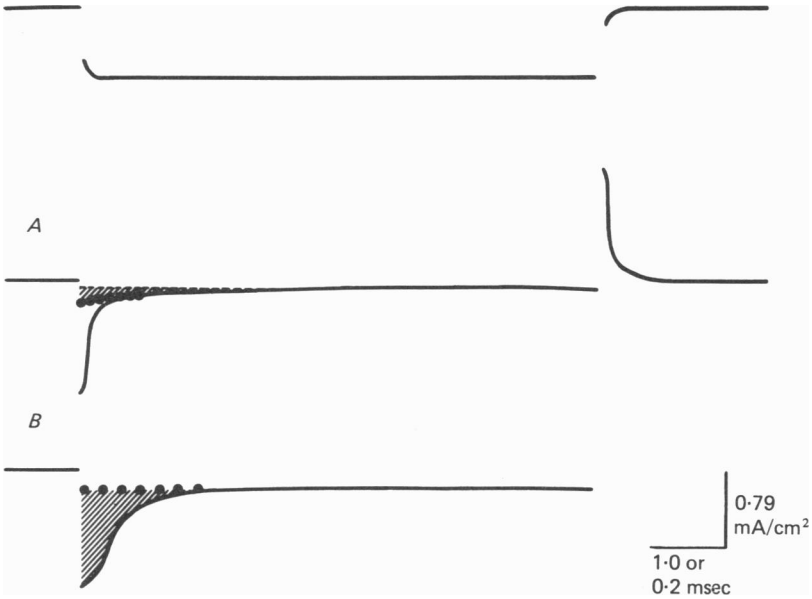

Fig. 3. Records of voltage (top) and current during a hyperpolarizing voltage-clamp step from the holding potential of −90 mV to −137 mV. *A*, horizontal line shows final, steady-state level of current, I_{ss}. Dots are calculated from an exponential function with time constant, $\tau_s = 1{\cdot}70$ msec and initial amplitude $I_s(0) = 0{\cdot}16$ mA/cm², fitted to the slow component of the current transient. Shaded area represents the charge movement used to calculate the slowly charging component of the capacity, C_s. *B*, current during the same voltage step as *A* on a faster time scale. Points as in *A*. Shaded area represents the charge movement used to calculate the rapidly charging component of the capacity, C_f. All records filtered at 4 KHz. Fibre 1/5/4, innervated e.d.l., 20 °C. Ends cut in CsF. Balance zero method. Calibration 1·0 msec in *A*, 0·2 msec in *B*.

membrane resistance of 826 Ωcm² and a specific membrane capacitance of 5·87 μF/cm² before contraction. The passive membrane properties reported here are in accord with previous results from cable analysis (Kiyohara & Sato, 1967; Zolovick, Norman & Fedde, 1970) and from voltage-clamp studies (Adrian & Marshall, 1977; Duval & Leóty, 1978), of intact rat muscle fibres.

Sodium current activation. Fig. 4 shows currents in an innervated s.m. fibre cut in CsF. Under these conditions, the delayed current is absent and only a transient inward current remains. The current is activated by depolarizations to potentials more positive than −80 to −70 mV and is carried by sodium ions (see below). The potential at which the sodium current reached a maximum was $-30{\cdot}6 \pm 2{\cdot}4$ mV

(mean ± S.E. of mean, $n = 10$) in innervated s.m. fibres, $-29{\cdot}0 \pm 1{\cdot}8$ mV ($n = 8$) in innervated e.d.l., and $-39{\cdot}8 \pm 1{\cdot}6$ mV ($n = 10$) in denervated e.d.l. The internal potential was not measured with micro-electrodes in these experiments, but the reversal potential of the sodium currents was the same in innervated and denervated e.d.l. fibres, being $+42{\cdot}3$ mV ($\pm 4{\cdot}2$ mV, $n = 8$) and 42·9 mV ($\pm 1{\cdot}9$ mV, $n = 8$), respectively. The internal sodium concentration of intact rat fibres does not change following denervation (Robbins, 1977; Creese, El-Shafie & Vrbová, 1968) so no change in the sodium reversal potential is expected. It seems unlikely therefore that

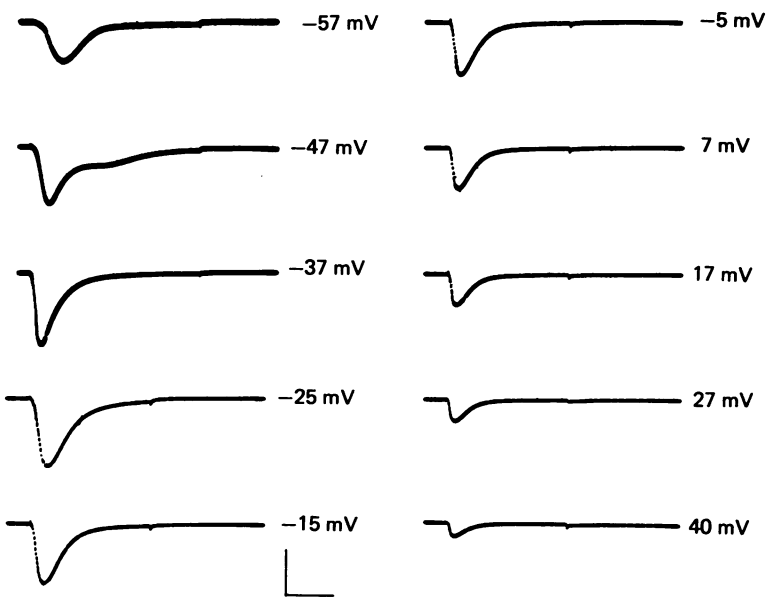

Fig. 4. Sodium currents in an innervated s.m. fibre with ends cut in CsF. Fibre depolarized to potential shown following a 50 msec hyperpolarization to −145 mV from the holding potential of −100 mV. Time calibration is 4 msec for traces at −57 mV, −47 mV and −37 mV, and 2 msec for all other traces. Current calibration is 1·8 mA/cm² for trace at −57 mV and 3·5 mA/cm² for all other traces. $T = 11$ °C. Fibre 12/23/3. Ends cut in CsF. Balance B − C method. The rising phase of some current records was retouched.

the difference in the potential of maximum current in innervated and denervated e.d.l. is due to errors in balancing amplifier A1. The values of the maximum peak current were $6{\cdot}8 \pm 1{\cdot}0$ mA/cm² ($n = 10$) in innervated s.m., $3{\cdot}8 \pm 0{\cdot}5$ mA/cm² ($n = 8$) in innervated e.d.l., and $6{\cdot}6 \pm 1{\cdot}3$ mA/cm² ($n = 10$) in denervated e.d.l. If the relative proportions of sarcolemma and tubular membranes remain the same, these values would correspond to 4·3 mA/cm² in s.m., 2·4 mA/cm² in innervated e.d.l., and 4·2 mA/cm² in denervated e.d.l. in uncontracted fibres. Even these corrected values are larger than calculated by Adrian & Marshall (1977) for intact rat e.d.l. fibres. This is like the situation in frog muscle where one also finds significantly larger sodium currents in cut fibres (Campbell & Hille, 1976) than in intact (Adrian *et al.*, 1970).

The sodium currents were analysed by fitting the current records by eye with an equation of the form (Hodgkin & Huxley, 1952)

$$I_{Na}(t) = I_{Na,0}(1-e^{-t/\tau_m})^3 e^{-t/\tau_h} \quad (3)$$

where τ_m is the time constant for activation of the current and τ_h the time constant for inactivation, and $I_{Na,0}$ the maximum sodium current expected if there were no inactivation of the current. At most potentials the inactivation of the sodium current follows an approximately exponential time course. However, the initial peak of inward sodium current is sometimes followed by a second peak (see e.g. Fig. 4 at −47 mV), especially at higher temperatures (> 15 °C). Similar secondary current peaks have been reported in voltage-clamped frog muscle (Hille & Campbell, 1976; Mandrino, 1977) and they probably arise from active sodium currents known to be present in the membrane of the transverse tubular system (Costantin, 1970; Bastian & Nakajima, 1974). Calculations by Hille & Campbell (1976) suggest that in frog muscle these currents are too small relative to the surface sodium currents to affect significantly the measurements of gating time course during depolarizations positive to −45 mV. Only records without a secondary peak of current were used for the kinetic analysis. Fig. 5 (top) shows the time constants for activation of sodium currents at 12 °C in normal and denervated e.d.l. fibres. No difference between the fibre types is apparent. Innervated s.m. and e.d.l. fibres also had similar time constants (not shown). The curve in Fig. 5 (top) is calculated from the model discussed below using the parameters for rat muscle given in Table 5.

The points in Fig. 5 (bottom) show averaged values of m_∞^3 in normal and denervated e.d.l. fibres. The parameter m_∞^3 was calculated from the relation

$$m_\infty^3 = I_{Na,0}/\bar{G}_{Na}\,(V-V_{Na}), \quad (4)$$

where V is the membrane potential, V_{Na} is the reversal potential for the sodium current, and $\bar{G}_{Na}$ is the maximum sodium conductance expected if all the channels were open. $\bar{G}_{Na}$ averaged $123 \pm 27{\cdot}8$ m-mho/cm² ($n = 4$) in innnervated e.d.l. and $107 \pm 18{\cdot}8$ m-mho/cm² ($n = 3$) in denervated e.d.l. measured at 12 °C. The curve in Fig. 5 (bottom) is calculated as above.

Both the peak sodium conductance and $\bar{G}_{Na}$ decline for potentials positive to −10 mV, producing a decline in the experimental m_∞ values. This decline is still evident if one analyses the data in terms of the Goldman–Hodgkin–Katz equation (Goldman, 1943; Hodgkin & Katz, 1949) rather than assuming an ohmic behaviour for an open sodium channel.

The activation of sodium current is shifted by approximately 10 mV to more hyperpolarized potentials in the denervated fibres compared to normal. In innervated e.d.l. fibres, the relative peak sodium conductance was half maximal at −52·1 mV (± 1·9 mV, $n = 8$). A similar value of −55·0 mV (± 1·2 mV, $n = 3$) was found in innervated s.m. fibres in which the internal potential was measured with a microelectrode. These values are somewhat more negative than the value of −47 mV reported by Adrian & Marshall (1977) for intact e.d.l. fibres in low sodium solutions. In denervated e.d.l., the potential at which the peak conductance was half maximal was significantly more negative ($P < 0{\cdot}005$) averaging −62·7 mV (± 1·8 mV, $n = 10$).

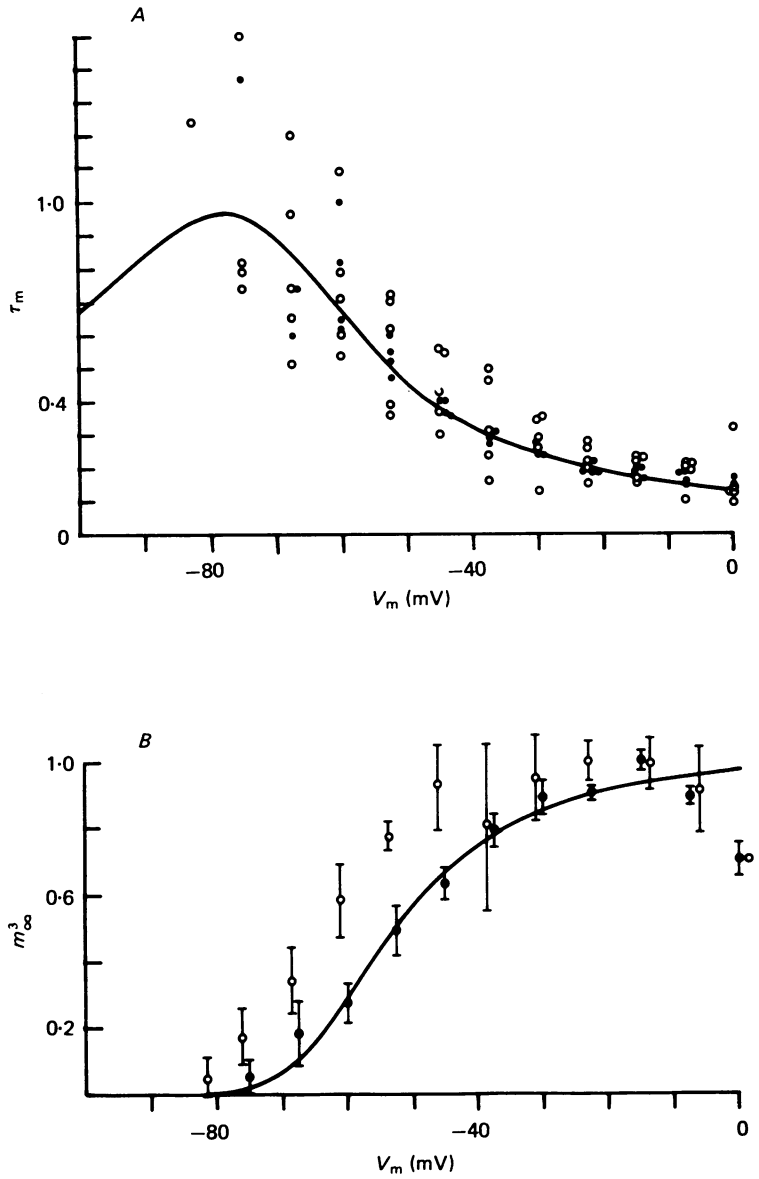

Fig. 5. A, τ_m as a function of membrane potential in innervated (filled symbols) and denervated (open symbols) e.d.l. fibres at 12 °C. Points calculated from fit of eqn. (3) to currents during depolarization to the potential on the abscissa following a 200 msec conditioning polarization to −135 mV. Curve calculated from eqn. (7) with parameters listed in Table 5. *B*, m^3_∞ as a function of voltage. Points calculated from some of the same current records as *A* using eqn. (4). Filled symbols: mean ± S.E. of mean from four innervated e.d.l. fibres. Open symbols: mean ± S.E. of mean from three denervated e.d.l. fibres. Curve calculated from eqn. (5) with the parameters listed in Table 5. Fibre ends cut in CsF. Balance zero method.

Maximum peak sodium conductances measured in innervated e.d.l. and s.m. fibres and in denervated e.d.l. fibres are listed in Table 2. There is no difference in the maximum peak conductance between innervated and denervated fibres at 12 °C. At 22 °C, the peak conductance was somewhat higher in denervated e.d.l. than in the normal fibres.

TABLE 2. Maximum peak sodium conductances

Fibre type	T	$G_{Na,max}$ m-mho/cm²	n
Innervated s.m.	12°	54·9 ± 11·9	6
	22°	68·0 ± 20·2	7
Innervated e.d.l.	12°	42·3 ± 5·7	4
	22°	74·5 ± 17·8	4
Denervated e.d.l.	12°	52·8 ± 5·1	5
	22°	139·0 ± 12·3	5

Maximum peak sodium conductance, $G_{Na,max}$ was calculated as $I_p/(V-V_{Na})\ \pi dl$ where V is the membrane potential, V_{Na} the sodium reversal potential, I_p the peak sodium current, d the fibre diameter and l the length of fibre in the A pool. Average values given ± S.E. of mean.

Inactivation of sodium current. As is well known, the increase in sodium current upon depolarization is followed by a relatively slower decline (e.g. Fig. 4), termed inactivation. A time constant of inactivation, τ_h, can be measured by fitting a single exponential to the decline of sodium current. Only records showing no secondary peak of inward current (as, e.g. in Fig. 4, −25 mV) were analysed, and signs of a slow phase of inactivation (Chiu, 1977) were ignored. Fig. 6 (top) shows τ_h as a function of voltage in innervated and denervated e.d.l. fibres and in innervated frog semitendinosus fibres, all at 12 °C. Inactivation rates are similar in all three preparations. In particular, Fig. 6 gives no indication that inactivation in the rat is slower than in the frog, as reported by Adrian & Marshall (1977) for intact muscle fibres.

The temperature dependence of τ_h was measured in two fibres (Table 3). A Q_{10} of 2–3 can be calculated from these data.

Fig. 6. (bottom) also plots the peak conductance during a fixed test pulse following a 100–200 msec conditioning pulse to various potentials. Experiments of this kind are normally used to measure the steady-state potential dependence of the inactivation parameter, h_∞. As in other excitable tissues, more Na^+ conductance can be elicited as the conditioning potential is made more negative, but in these experiments a saturating level is not obtained even with conditioning pulses as negative as −120 mV. Furthermore, the curves seem shifted to more negative potentials compared to those obtained in intact fibres. In innervated fibres, for instance, the fractional sodium conductance available at the physiological resting potential (−80 mV) is 20 % in Fig. 6, compared to about 50 % for intact fibres found by Adrian & Marshall (1977) or Duval & Leóty (1978). In denervated fibres, the curve is shifted to even more negative potentials; at −90 mV, the holding potential in these experiments, the difference between innervated and denervated fibres is statistically significant at the $P < 0{\cdot}005$ level. Results similar to those of Fig. 6 (bottom) were obtained from fibres cut in glutamate plus K_2 EGTA, with and without 5 mM-ATP inside, in oxygenated fibres, and in fibres in which the internal potential was verified

by micro-electrode measurement. During some experiments, the inactivation curve spontaneously shifted to more negative potentials. There was, however, no change in the time constant for inactivation of sodium current during depolarization or in the voltage dependence of sodium current activation accompanying the shift in steady-state inactivation.

TABLE 3. Temperature dependence of sodium current inactivation

		τ_h (msec)		
Fibre	T (°C)	−57 mV	−13 mV	+43 mV
10:13:2	20°	2·47	0·49	0·21
	11°	4·18	0·79	0·65
	20°	2·20	0·51	0·23
10:13:3	20°	1·98	0·32	0·22
	10°	3·65	1·06	0·52
	20°	1·98	0·45	0·26

Experiments performed in order shown. Fibres from the same innervated s.m. muscle. Fibres allowed to equilibrate for at least 5 min at each temperature. Balance set using microelectrode measurement of V_D following equilibration period. Ends cut in CsF.

In comparing the present results to those in intact fibres, one must consider that the maximum conductances observed here are two to three times larger than those observed by Adrian & Marshall (1977) and Duval & Leóty (1978), so, in absolute terms, the sodium conductance available after a prepulse to −80 mV may have been similar in this and previous work. I nevertheless feel that the curves in Fig. 6 (bottom) do not reflect accurately the physiological equilibrium distribution between the resting state and Hodgkin & Huxley's (1952) inactivated state. This may be in part a peculiarity of my cut fibres, but could also be due to slow inactivation processes which do not reach equilibrium during a 200 msec conditioning pulse.

Fig. 7 (top) illustrates a procedure which should be less sensitive to contamination by slow inactivation. A 50 msec conditioning pulse to the potential V_C (−57 mV in Fig. 7, top) was applied, the fibre was allowed to recover at −100 mV for various times, and the extent of recovery was assayed with a test pulse to V_T. I_1 is the current during a test pulse given without recovery interval and should be proportional to the number of activatable channels remaining at the end of the conditioning pulse. I_2 (dashed line) is the level reached after fast recovery processes (such as are expected to govern recovery from Hodgkin-Huxley type inactivation) have gone to completion. Sometimes the current during the test pulse continued to grow over the entire recovery period of 500 msec; in that case, a single exponential was fitted to the data points obtained with longer recovery intervals (> 200 msec) and extrapolated to zero time to give I_2. Insofar as a 50 msec conditioning pulse is enough to bring rapid inactivation to equilibrium, the ratio I_1/I_2 gives the equilibrium distribution between resting and rapid inactivated states independent of states governed by slower processes, and should correspond to the variable h_∞ of Hodgkin & Huxley (1952). Fig. 7 (bottom) plots I_1/I_2 against V_C (filled symbols). The relationship is more similar to the results on intact fibres than the curve in Fig. 6 (bottom). Slow recovery from inactivation is also seen in intact fibres at low temperature (< 15 °C).

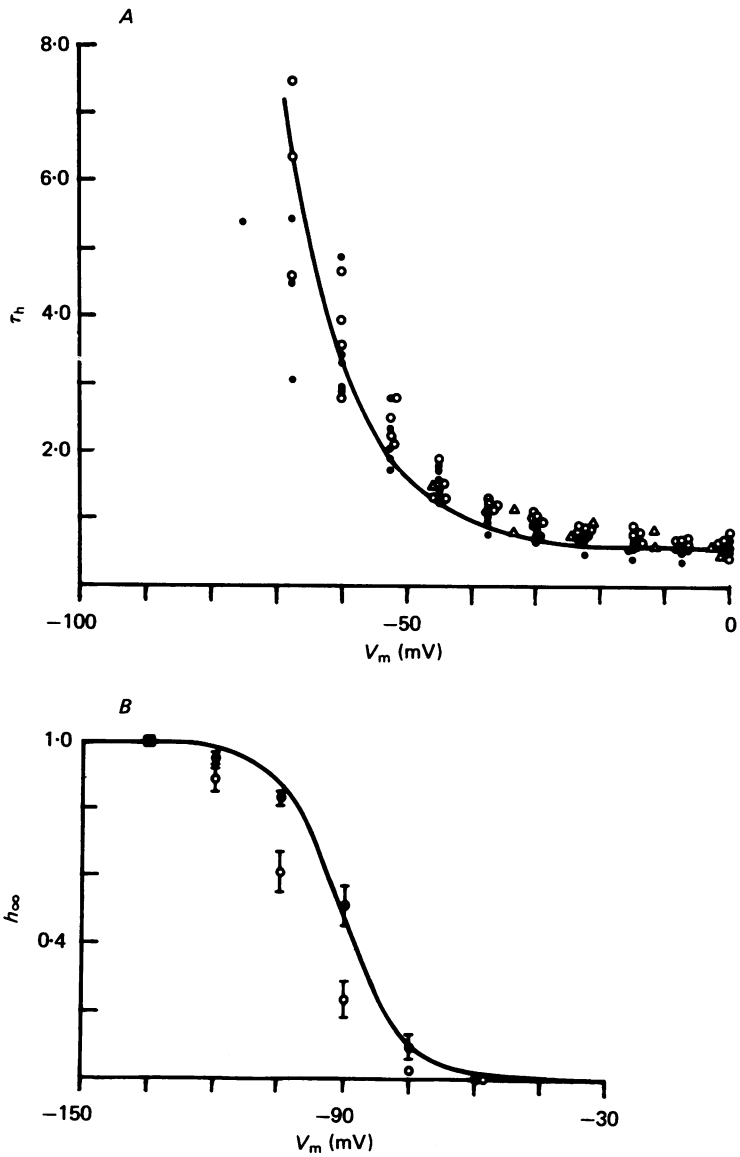

Fig. 6. Top: time constants of sodium current inactivation, τ_h, as a function of membrane potential in innervated (○) and denervated (●) rat e.d.l. fibres and in innervated frog semitendinosus muscle (△), all at 12 °C. τ_h is the time constant of a single exponential fitted to the decline of sodium current during depolarization. Curve calculated from eqn. (8) with parameters listed for rat muscle in Table 5. Bottom: voltage dependence of inactivation in seven innervated (filled symbols) and eight denervated (open symbols) e.d.l. fibres. The level of inactivation was measured at the end of a 200 msec (experiments at 12 °C) or 100 msec (experiments at 20 °C) conditioning pulse on the peak sodium current during a test pulse to near 0 mV. Values normalized to the peak current following a conditioning pulse to −135 mV (■). Error bars give S.E. of mean. Curve calculated from eqn. (6) with the parameters listed for rat muscle in Table 5. Fibres cut in CsF. Balance zero method. Holding potential −90 mV.

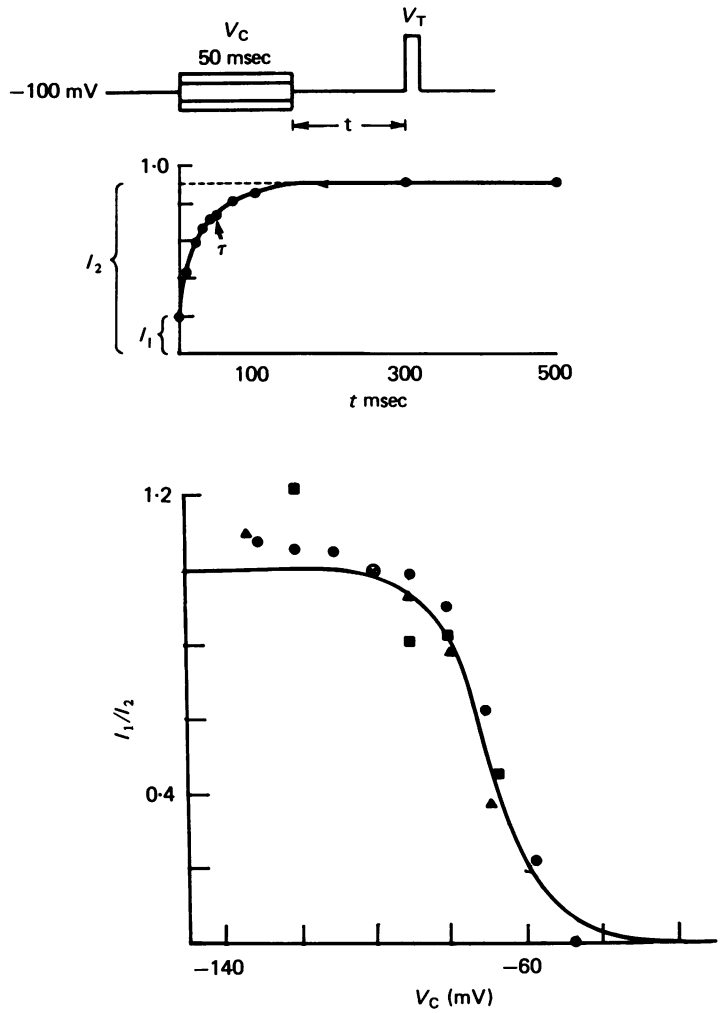

Fig. 7. Top: separation of fast and slow recovery at −100 mV from inactivation by a 50 msec conditioning pulse to −57 mV. Peak sodium current during a test pulse to +7 mV (I_T), as a fraction of that without a conditioning pulse (I_C), is plotted against the interval between the end of the conditioning and the beginning of the test pulse. I_1 and I_2 are defined in the text. The time constant for the fast portion of recovery (τ_1) was 48 msec. 30 sec wait between pulses. Fibre 12/3/3, 11 °C. Ends cut in CsF. Balance B−C method. Bottom: I_1/I_2 as a function of conditioning potential, V_C. Each symbol type represents data from a different fibre. Curve calculated from eqn. (6) with the parameters for frog muscle listed in Table 5. Ends cut in CsF. 11 °C. Balance B–C method.

Stimulation at 5 Hz produced action potentials with successively decreasing rates of rise in this temperature range. Intact fibres at 20 °C could follow stimulus frequencies of 10 Hz with no change in the shape of the action potential.

The 50 msec duration of the conditioning pulse seems short compared to an average recovery time constant of $40 \pm 5{\cdot}0$ msec ($n = 5$) at −100 mV and 12 °C. However, it should be sufficient at more positive potentials. In all three fibres represented in Fig. 7, inactivation during a pulse

from -100 mV to -70 mV could be measured directly from the decline of the small sodium currents elicited at that potential; τ_h was <15 msec in all cases. As far as more negative potentials are concerned, it is not clear whether inactivation and recovery represent the same processes. In one fibre, the temperature dependence of recovery at -100 mV was measured and indicated a Q_{10} of 4·1, nearly twice that observed for the development of inactivation. Furthermore, Nonner (1978) showed that at a given negative potential, recovery can be up to three times slower than development of inactivation. Thus, the large recovery time constant of 40 msec at -100 mV may cast some doubt on the data at more negative potentials, but at more positive potentials one may consider that the data are reasonably accurate representations of the equilibrium distribution between the resting and the quickly reached inactivated state.

TABLE 4. Equations for rate constants of sodium currents

$$\alpha_m = \frac{\bar{\alpha}_m (V-\bar{V}_m)}{1-\exp[-(V-\bar{V}_m)/k_{\alpha,m}]} \qquad \alpha_h = \bar{\alpha}_h \exp[-(V-\bar{V}_h)/k_{\alpha,h}]$$

$$\beta_m = \bar{\beta}_m \exp[-(V-\bar{V}_m)/k_{\beta,m}] \qquad \beta_h = \frac{\bar{\beta}_h}{1+\exp[-(V-\bar{V}_h)/k_{\beta,h}]}$$

TABLE 5. Parameters of kinetic model of sodium currents in innervated rat and frog muscle

	Rat muscle (12 °C)	Frog muscle
$\bar{\alpha}_m$ (msec^{-1})	0·115	0·098
$\bar{\beta}_m$ (msec^{-1})	0·55	1·13
$\bar{V}_m$ (mV)	−63·5	−42·0
$k_{\alpha,m}$ (mV)	6·8	10·0
$k_{\beta,m}$ (mV)	37	18·0
$\bar{\alpha}_h$ (msec^{-1})	0·00323	0·00029
$\bar{\beta}_h$ (msec^{-1})	1·75	2·21
$\bar{V}_h$ (mV)	−46	−25
$k_{\alpha,h}$ (mV)	25	11·0
$k_{\beta,h}$ (mV)	10	13·6

Parameters for activation and inactivation in rat muscle chosen to fit data from innervated e.d.l. fibres at 12 °C. Frog muscle parameters are from the model of Campbell & Hille (1976) at 5 °C with rate constants scaled to 12 °C by a factor of 2·45, equivalent to Q_{10} of 3·6.

Kinetic model of sodium currents. The sodium currents of mammalian muscle are similar to those of frog muscle, and the empirical models which have been developed for frog muscle sodium channel gating can be used to describe the kinetics of sodium currents in mammalian muscle with minor modification. The experimentally determined parameters m_∞, h_∞, τ_m, and τ_h are defined in terms of rate constants by the following equations

$$m_\infty = \alpha_m/(\alpha_m+\beta_m), \tag{5}$$

$$h_\infty = \alpha_h/(\alpha_h+\beta_h), \tag{6}$$

$$\tau_m = 1/(\alpha_m+\beta_m), \tag{7}$$

$$\tau_h = 1/(\alpha_h+\beta_h). \tag{8}$$

The rate constants calculated from the above equations were fitted with functions of the form used by Adrian *et al.* (1970) and Campbell & Hille (1976) for frog muscle shown in Table 4. Average values of the parameters determined for innervated e.d.l.

fibres are shown in Table 5 along with those from Campbell & Hille's (1976) study of frog fibres. The values of m_∞, τ_m, h_∞, and τ_h calculated for innervated e.d.l. are shown in Figs. 5 and 6.

The model was used to calculate membrane action potentials in innervated muscle fibres. The tubular membrane was modelled by the equivalent circuit

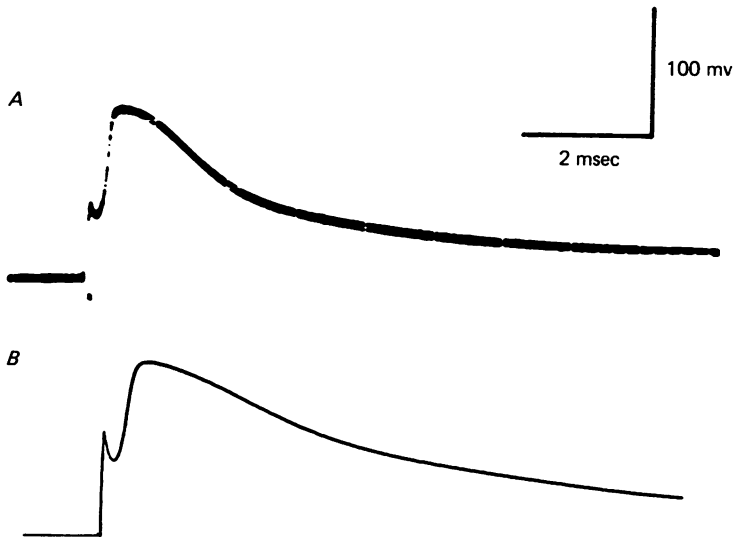

Fig. 8. *A*, membrane action potential recorded in the vaseline gap. Starting potential was −100 mV. Fibre 9/28/3. Ends cut in CsF. *B*, calculated membrane action potential. Action potential was calculated from the parameters in Table 5 as described in the text with $\bar{G}_{Na} = 125$ m-mho/cm², $E_{Na} = +45$ mV, $E_L = -90$ mV. Starting potential was −100 mV.

proposed by Falk & Fatt (1964). Values of R_s, R_t, C_s and C_t were extrapolated from the passive properties reported here to simulate the analysis of rat muscle in terms of the Falk & Fatt model in contracted cut fibres (Duval & Leóty, 1978). All sodium current was assumed to be carried through the surface membrane.

Fig. 8 shows a membrane action potential calculated using the parameters for rat muscle in Table 5. Also shown is an action potential recorded from one of the fibres used in the kinetic analysis, with potassium currents blocked by internal Cs. The calculated action potential resembles that recorded in the vaseline gap in threshold, rate of rise, amplitude and rate of repolarization. In both the calculated and recorded action potentials the rate of repolarization is slow, as is expected in the absence of potassium currents. If the h_∞ relation is shifted to more positive potentials to more closely approximate that measured in intact fibres, the calculated action potential fails to repolarize completely. Under these conditions there is a stable resting potential at −60 mV. The kinetic model presented here accurately predicts the behaviour of rat fibres under current clamp in the vaseline gap.

Selectivity of sodium channels. The permeability, P_s, of the sodium channel to several monovalent cations was compared to the sodium permeability, P_{Na}, by determining the change in reversal potential of the early current when all the exter-

nal sodium was replaced by the test cation. Following Hille (1971), the permeability ratio, P_s/P_{Na}, can be obtained from

$$V_s - V_{Na} = \frac{RT}{F} \ln \frac{P_s[S^+]}{P_{Na}[Na^+]}. \quad (9)$$

Here V_{Na} and V_s are the reversal potentials for the early current in the control and test solutions, respectively, $[Na^+]$ and $[S^+]$ are the concentrations of Na^+ and

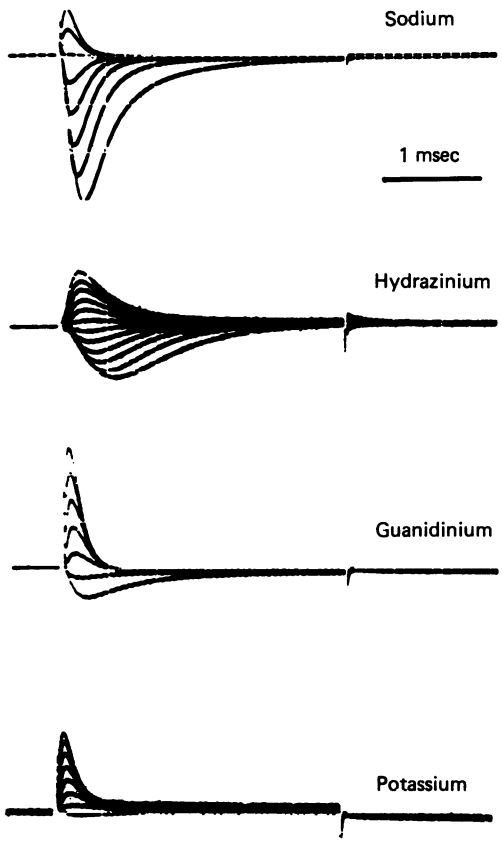

Fig. 9. Currents in Na Ringer solution and in solutions with Na replaced by hydrazinium, guanidinium, or potassium. Fibre ends cut in CsF. Innervated s.m. Fibre 7/30/4, 12 °C. Balance B–C method.

the test ion, and R, T, and F have their usual meanings. Test runs were bracketed by control runs, and V_s compared to the average V_{Na} of the bracketing controls.

Fig. 9 shows current from a series of step depolarizations in normal Ringer solution and after replacing all of the Na^+ with hydrazinium, guanidinium, or potassium. There are inward currents through the sodium channels in all cases, indicating that all these ions are permeant. Fig. 10 shows the peak current–voltage relations obtained from the records of Fig. 9.

Table 6 shows the permeability ratios for the sodium channels of rat s.m. fibres compared with those of frog muscle from the experiments of Campbell (1976).

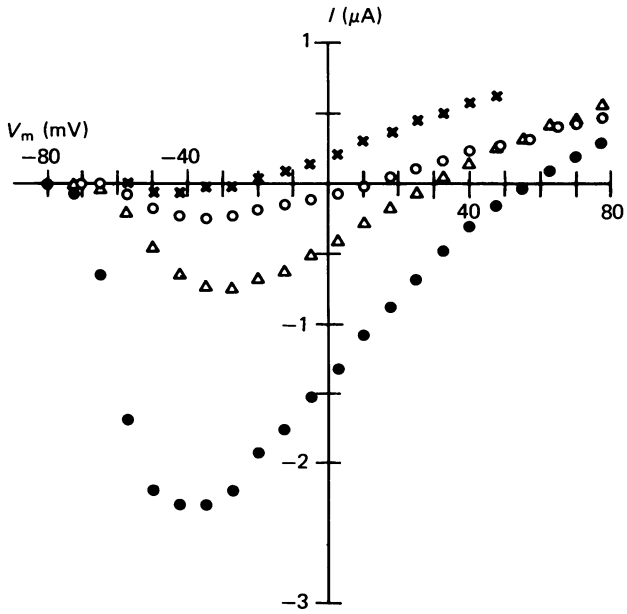

Fig. 10. Peak currents as a function of voltage in Na Ringer (●), hydrazinium Ringer (△), guanidinium Ringer (○) and K Ringer solution (×). Same fibre as Fig. 9.

TABLE 6. Sodium channel selectivity

Ion	$[S^+]/[Na^+]$	$V_s - V_{Na}$	Rat muscle P_s/P_{Na}	Frog muscle P_s/P_{Na}
Lithium	1·02	+ 3·0	1·14	0·96
	.	± 1·9	± 0·08	.
Hydroxylammonium	0·43	− 23·3	0·90	0·94
	.	± 0·3	± 0·01	.
Hydrazinium	1·10	− 29·2	0·30	0·31
	.	± 2·9	± 0·04	.
Guanidinium	1·00	− 46·2	0·16	0·093
	.	± 1·3	± 0·04	.
Ammonium	1·00	− 47·8	0·15	0·11
	.	± 1·6	± 0·01	.
TMA	1·00	> − 99·0	< 0·012	0·008
	.	± 16·0	± 0·002	.
Potassium	0·99	− 80·7	0·045	0·048
	.	± 8·2	± 0·014	.

$[S^+]/[Na^+]$ for Li^+ and K^+ are activity ratios, calculated by using ratios of activity coefficients taken from Robinson & Stokes (1965). Activity coefficients of organic cations assumed equal to that of Na. $[S^+]$ for hydroxylammonium and hydrazinium calculated from the total concentration assuming pK_a values of 5·95 and 7·97 respectively. pH of the hydroxylammonium Ringer solution was 5·78 and of the hydrazinium Ringer solution 6·00. All other solutions had pH 7·2–7·3. The K Ringer solution had SO_4^{2+} as the major anion and 60 mM-sucrose added to maintain isotonicity. Experiments were done at 12, 15 or 20 °C. Permeability ratios were calculated for individual experiments before averaging. Permeability ratios in frog muscle from Campbell (1976). Experiments in rat muscle performed on innervated s.m. fibres with ends cut in CsF.

Permeability ratios are essentially the same in the two species. Lithium and sodium were the most permeant of the ions tested, having approximately equal permeabilities. In contrast to the 20 % decrease seen in frog muscle (Hille, 1972; Campbell, 1976), in rat muscle there is no reduction in the size of the currents in Li^+-Ringer compared to Na^+-Ringer solution. The only other measurably permeant univalent

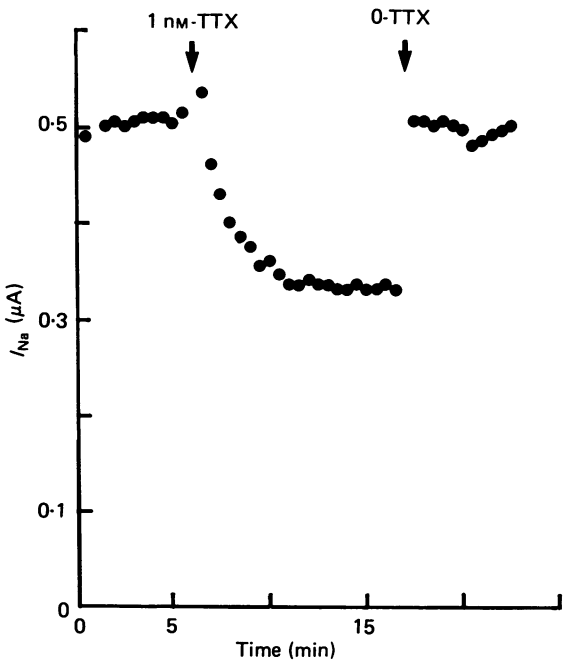

Fig. 11. Time course of block of sodium current in an innervated s.m. fibre at 13 °C. Peak amplitude of the sodium current during a depolarization to 0 mV following a conditioning pulse to −112·5 mV for 100 msec. Fibre initially in toxin-free Ringer solution. At 6 min the solution in the A pool was changed to Ringer + 1 nM-TTX. At 17 min the toxin was washed out. Fibre 8/22/7. Ends cut in CsF. Balance zero method.

inorganic cation tested was potassium. P_K/P_{Na} was 0·048, similar to the value for frog muscle. When Ca^{2+} replaced Na^+, no inward currents were seen.

Of all the organic cations tested, hydroxylammonium was the most permeant, being almost as permeant as sodium. The currents in hydroxylammonium Ringer solution are half the size one would expect from the same concentration of sodium, however. Some of this difference may be due to block of the channels by H^+, since the test solution had pH 5·8. If rat sodium channels have the same pK_a as frog, one would expect 20 % of the channels to be blocked at this pH. Hydroxylammonium itself may also block the channels. Hydrazinium, guanidinium and ammonium were also permeant. Tetramethylammonium (TMA) was impermeant, showing no inward currents. The upper limit for the permeability ratio of TMA^+ is 0·012.

Effect of tetrodotoxin

Innervated muscle. TTX applied in nanomolar concentrations reduced the amplitude of sodium currents in voltage-clamped innervated and denervated rat muscle fibres. In Fig. 11, 1 nM-TTX rapidly and reversibly reduced the peak amplitude of the current to 70 % of its control value. Unfortunately, the time course of changes in the peak sodium current in Fig. 11 is not determined solely by the rate of reaction

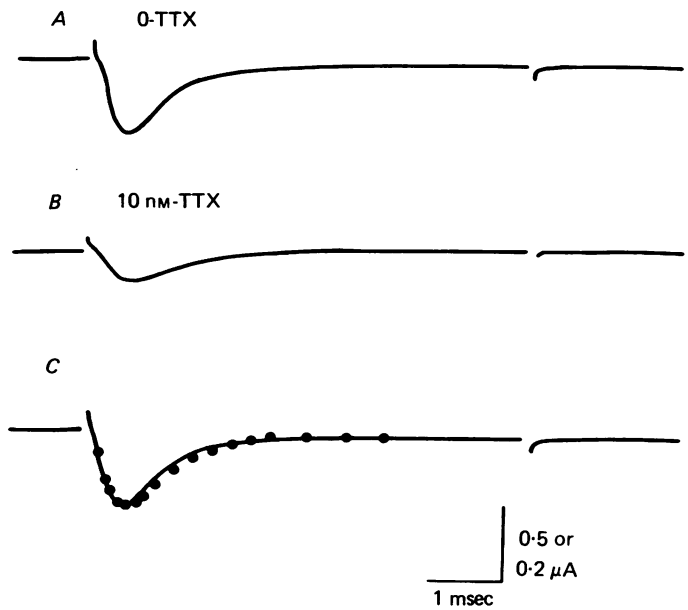

Fig. 12. Sodium currents in an innervated e.d.l. fibre at 12 °C during a test pulse to −10 mV following a conditioning pulse to −140 mV for 200 msec. A, toxin-free Ringer solution. *B*, Ringer solution +10 nM-TTX. *C*, continuous curve same as *A*; points are from record *B* scaled by a factor of 5·2 to have the same peak amplitude as record *A*. Ends cut in CsF. Fibre 9/27/4. Balance zero method.

of TTX with its receptor. Washout of a fibre bathed in Ringer solution with more Ringer often results in an unexplained transient increase in the amplitude of the sodium current, and even in Fig. 11 the first measurement following the wash with TTX shows a larger sodium current than the control. However, the experiment shows that a wait of 5 min should be sufficient for the toxin–receptor reaction to reach equilibrium.

TTX decreases the amplitude of the sodium current in innervated rat muscle without affecting either the time course (Fig. 12) or the voltage dependences of peak conductance and steady-state inactivation. Fig. 12 shows the sodium current in an innervated e.d.l. fibre. TTX reduced the peak amplitude to 18 % of its control value. The kinetics of the current are not significantly altered. In twenty-eight experiments of this kind, the time-to-peak never changed by more than 10 %. As in nerve (Hille, 1968), TTX seems to block sodium channels without affecting the properties of the remaining unblocked channels.

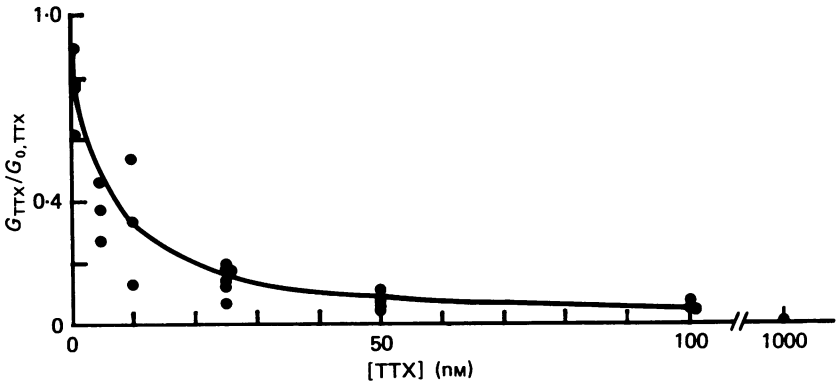

Fig. 13. Dose–response relation for sodium conductance in TTX in innervated e.d.l. fibres. Points represent the ratio of the peak conductance in TTX, G_{TTX}, relative to the averaged values of the peak conductance without TTX, $G_{0,\,TTX}$, before and after application of toxin. Curve calculated from eqn. (10), with $K_1 = 5{\cdot}1$ nM.

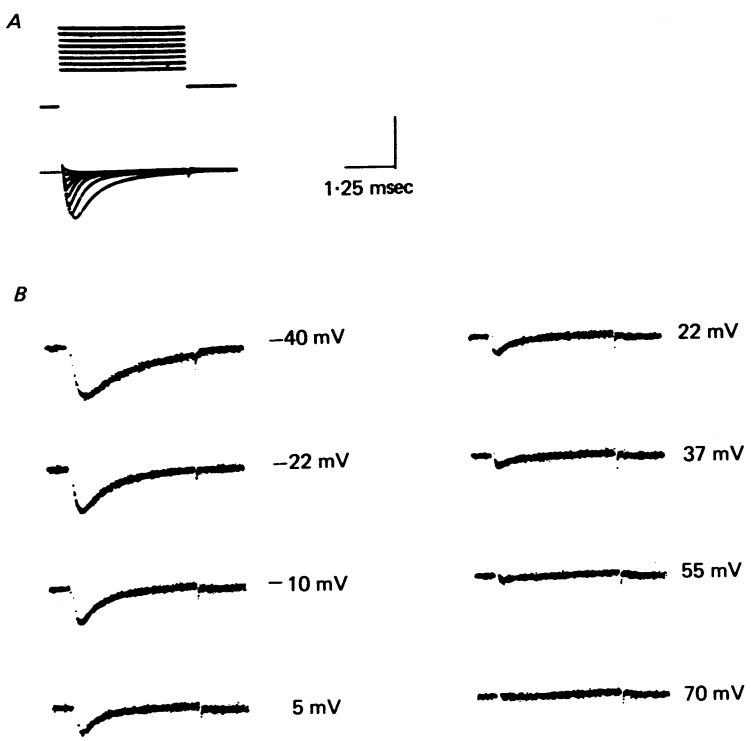

Fig. 14. *A*, sodium currents in a denervated e.d.l. fibre in Ringer solution without TTX. Fibre was depolarized to the potentials shown in *B* following a 100 msec conditioning prepulse to −137·5 mV. Current calibration 8·8 mA/cm². Fibre ends cut in CsF. Fibre 1/17/5. 23 °C. Balance zero method. *B*, currents in the same fibre in 100 nM-TTX during depolarization to the potentials shown. Same pulse protocol as *A*. Current calibration 1·8 mA/cm².

Fig. 13 shows the dose–response relationship for peak sodium conductance at around 0 mV. Peak conductances rather than peak current values were used in these calculations because of slight changes in reversal potential during experiments which were due, perhaps, to diffusional exchange of internal K^+ and Na^+ for the Cs^+ in the end pools. Peak conductances in TTX, G_{TTX}, are shown relative to the average of the

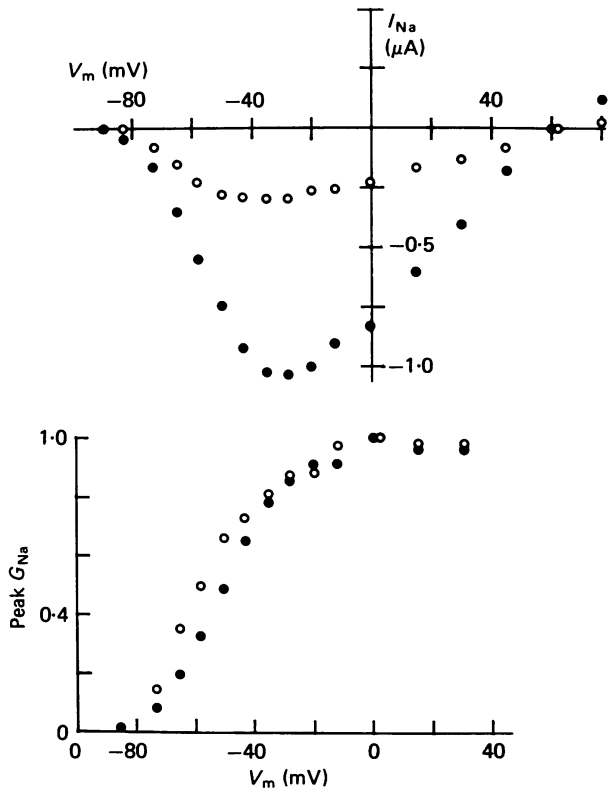

Fig. 15. Top: peak current–voltage relation in a denervated e.d.l. fibre without TTX (filled symbols) and in 100 nM-TTX (open symbols). Depolarization to potential shown preceeded by a 200 msec conditioning prepulse to −137·5 mV from the holding potential of −90 mV. Fibre ends cut in CsF. Fibre 9/19/1. 12 °C. Balance zero method. Bottom: normalized peak conductance–voltage relation from the same records. Symbols as above. Maximum peak conductance was 44·0 m-mho/cm² without toxin, 11·9 m-mho/cm² in 100 nM-TTX.

conductances in toxin-free solution at the same potential before and after application of toxin, $G_{0,TTX}$. The curve in Fig. 13 is calculated from the equation

$$G_{TTX}/G_{0,\,TTX} = \frac{K_1}{K_1+[TTX]}, \tag{10}$$

where K_1, the dissociation constant for TTX is 5·1 nM. The data are fitted well by this equation, consistent with the idea that there is a single class of sodium channels in innervated rat muscle, and that a single molecule of TTX is sufficient to block a channel.

Denervated muscle. Fig. 14 shows the currents in a denervated e.d.l. fibre before and after adding 100 nM-TTX. While 100 nM-TTX blocked 95% of the sodium current of innervated muscle, large currents of up to 35% of the control amplitude remain in the denervated fibre. Transient outward currents in 100 nM-TTX were too small to allow a reliable measurement of the reversal potential (e.g. at +70 mV

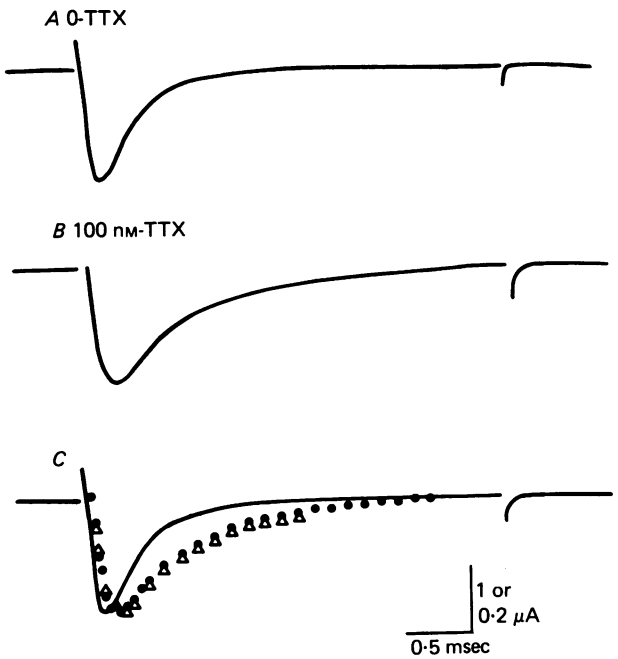

Fig. 16. Sodium currents in a denervated e.d.l. fibre during depolarization to −11·5 mV following a 100 msec conditioning prepulse to −137·5 mV. *A*, normal toxin-free Ringer solution, 1 μA current scale. *B*, Ringer +100 nM-TTX, 0·2 μA current scale. *C*, curve same as *A*. Filled circles are from record *B* scaled by a factor of 5 to have the same peak value as in *A*. Open symbols from current record in the same fibre in 1 μM-TTX at the same potential (not shown) scaled by a factor of 18·4. Same fibre as Fig. 14.

in Fig. 14); however, the general shape of the current–voltage curve in Fig. 15*A* suggests that, as in innervated fibres, TTX does not change the reversal potential. There is little doubt that the TTX-resistant currents in Fig. 14 are carried by Na^+, since they are abolished if all the external Na^+ is replaced by TMA^+ or by an isotonic mixture of Ca^{2+} (50 mM) and sucrose (one experiment each). Further preliminary experiments have shown TTX-resistant inward currents in Na^+-free Ringer solution containing hydroxylammonium or hydrazinium ions, so both these ions are permeant, as they are in innervated muscle.

Assuming the same reversal potentials with and without TTX, peak currents in TTX can be converted to peak conductances. Fig. 15*B* compares normalized peak conductance–voltage curves with and without toxin. In this experiment, the relation was somewhat shifted to more hyperpolarized potentials. This was not a consistent finding, and the fibre in Fig. 15*B* showed this effect to the greatest extent seen. The

toxin-resistant currents reach a peak amplitude and inactivate 1·5–3 times more slowly than the normal currents. This is shown in Fig. 16 which compares the time course of currents before and after adding TTX. In 100 nM-TTX, the time-to-peak and rate of inactivation are considerably slower than normal. However, increasing

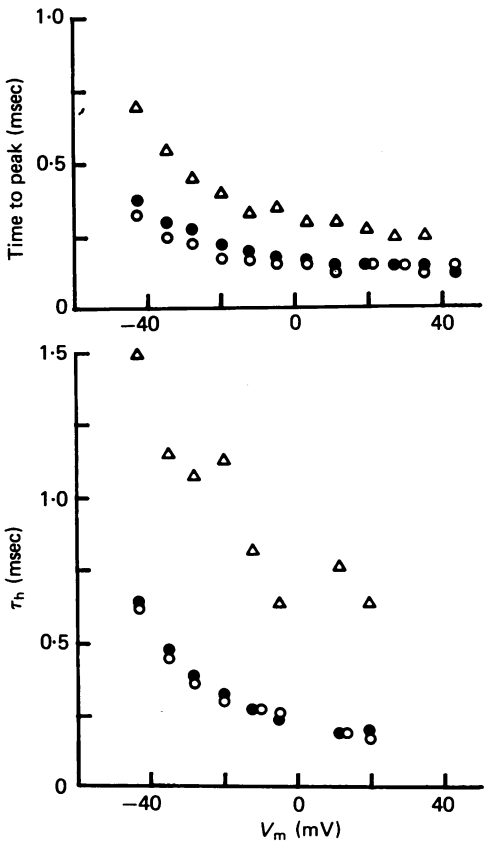

Fig. 17. Time-to-peak and time constants of inactivation (τ_h) in a denervated e.d.l. fibre. Triangles in 1 μM-TTX. Circles in toxin-free Ringer solution before (filled) and after (open) application of the toxin. Same fibre as in Figs 14 and 16.

the toxin concentration tenfold did not produce any further change in the time course of the current. During pulses to −10 mV, 100 nM-TTX increased the time-to-peak 1·7 ± 0·1 times (± S.E. of mean, $n = 7$) in denervated fibres. It is not likely that the change in kinetics is due to a current-dependent artifact, since no change was present in innervated fibres in which the current magnitude was reduced to a similar extent (see above). Nor is it likely to be caused by drifts in the preparation, since shifts of up to 60 mV would be required to produce a change in the kinetics of the magnitude seen, and because the effect was reversible on washout of the toxin (see Fig. 17).

It is possible that a slowing of the kinetics could occur if the channels carrying the TTX-resistant currents had the characteristics of normal channels, but were

preferentially located in the transverse tubular system (t.t.s.). However, my calculations of the currents expected from tubular sodium channels using the mesh model of the t.t.s. (Adrian, Chandler & Hodgkin, 1969) predict a faster rate of inactivation of tubular currents compared to surface currents in the threshold range of potentials. As is shown in Fig. 17, τ_h for the resistant currents is larger over the entire voltage range between -40 mV and $+40$ mV.

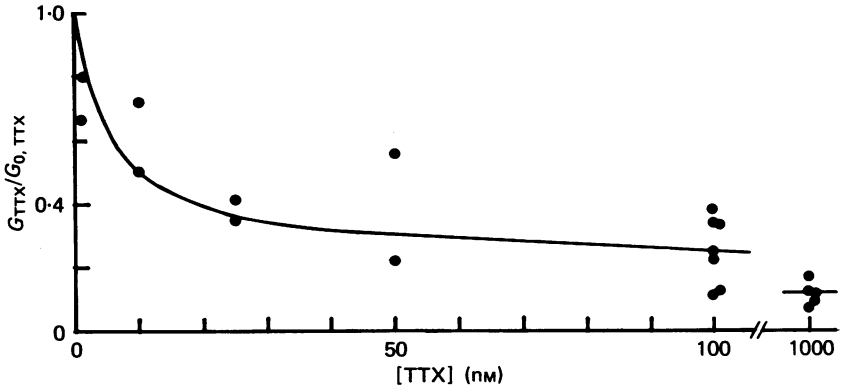

Fig. 18. TTX dose–response relation in denervated e.d.l. fibres. Curve is calculated from eqn. (11), with $K_1 = 5{\cdot}1$ nM, $K_2 = 1$ μM, and $A = 0{\cdot}75$.

The simplest interpretation of these results with TTX is to suppose that upon denervation a second type of sodium channel appears in the cell membrane, either from *de novo* synthesis or by modification of existing channels. This second type (Type II) is similar to ordinary sodium channels (Type I) in its voltage dependence and, possibly, its selectivity, but it shows sightly slower kinetics and greatly diminished sensitivity to TTX. This interpretation is consistent with previous work (Grampp, Harris & Thesleff, 1972; Ritchie & Rogart, 1977) and leads to the conclusion that the currents in Fig. 14*A* contain contributions from both types of channel, while those in Fig. 14*B* are due almost entirely to Type II channels, since Type I would be blocked by 100 nM-toxin.

Further support for the two-channel hypothesis comes from the toxin dose–response relation in denervated fibres (Fig. 18). The response to TTX was determined as follows: the time-to-peak of the current in a high concentration of TTX (0·1 or 1 μM) was measured. The current magnitude at this time was measured at the same potential in other concentrations of TTX and without TTX. These current values were used to calculate the conductance at this time in TTX, G_{TTX}, and without TTX, $G_{0,\ TTX}$. The resulting dose–response relation could not be fitted well assuming there was a single type of sodium channel in denervated fibres. The curve in Fig. 18 is calculated from the equation:

$$G_{TTX}/G_{0,\ TTX} = A\left[\frac{K_1}{K_1+[TTX]}\right] + (1-A)\left[\frac{K_2}{K_2+[TTX]}\right]. \qquad (11)$$

The first term on the right of eqn. (11) represents the response of Type I channels, with $K_1 = 5{\cdot}1$ nM. The second term represents the response of the Type II channels

with $K_2 = 1$ μM. The data could be best fitted with $A = 0{\cdot}75$. Since currents in the absence of TTX have declined to $0{\cdot}80 \pm 0{\cdot}02$ ($\pm$ S.E. of mean, $n = 8$) of their peak value at the time for the measurement, the Type II channels would be expected to contribute 0·25 times 0·8 of the peak conductance, or 20 %, in the absence of toxin. So Type I channels contribute about 4 times more peak conductance than Type II

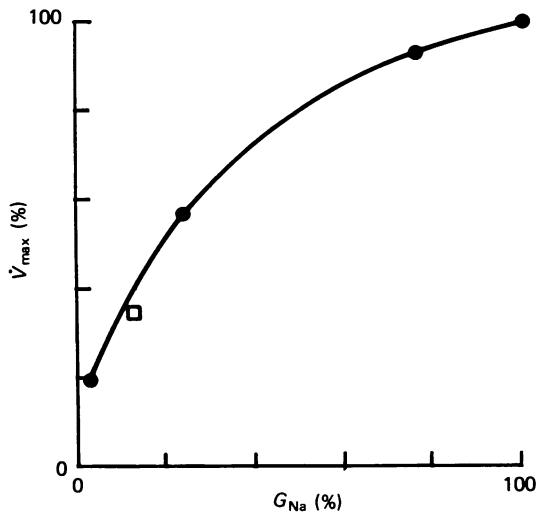

Fig. 19. Relation between the maximum rate of rise of the action potential, $\dot{V}_{max}$, and relative sodium conductance, % G_{Na}. Filled circles are from Harris & Thesleff's (1971) $\dot{V}_{max}$ data in intact innervated e.d.l. fibres in TTX combined with the expected G_{Na} calculated from eqn. (10) with $K_1 = 5{\cdot}1$ nM. Open square shows relative $\dot{V}_{max}$ in intact denervated e.d.l. in relation to the % G_{Na} found in the present experiments, both measured in 1 μM-TTX.

channels. The relative conductance of the Type II channels may be somewhat higher in intact fibres. In a later series of experiments, denervated fibres often failed to show toxin-resistant sodium currents in the vaseline gap preparation, in spite of the fact that TTX-resistant action potentials were consistently present in intact fibres.

Approximately 12 % of the normal sodium conductance in denervated fibres remains in 1 μM-TTX. However, the maximum rate of rise of the action potential, $\dot{V}_{max}$, of intact fibres is reduced only to 35 % of its control value by this concentration of toxin. This is due to the non-linearity of the relation between relative sodium conductance and $\dot{V}_{max}$ in rat muscle. Fig. 19 shows the conductance data from the present experiments in innervated muscle in relation to the $\dot{V}_{max}$ dose–response data for TTX from the experiments of Harris & Thesleff (1971), also on innervated muscle. Also included is a measurement of $\dot{V}_{max}$ in 1 μM-toxin after denervation; it falls on the same curve as the data on innervated fibres. Evidently, 10 % of the normal sodium conductance is sufficient to produce an action potential with 35 % of the normal $\dot{V}_{max}$.

Delayed currents. Delayed outward currents similar to those in nerve and frog skeletal muscle can be recorded also from rat muscle fibres (Fig. 20). As in other

tissues, they are probably carried by K^+. They are absent if the end pools contain TEA^+ or Cs^+, suggesting that these ions block delayed currents in rat as they do in frog skeletal muscle (Fink & Weltwer, 1978) and frog myelinated nerve (Armstrong & Hille, 1972). Because the currents in Fig. 20 are pharmacologically and kinetically so similar to delayed K^+-currents in nerve and frog skeletal muscle, I assume that they too are carried by K^+ ions.

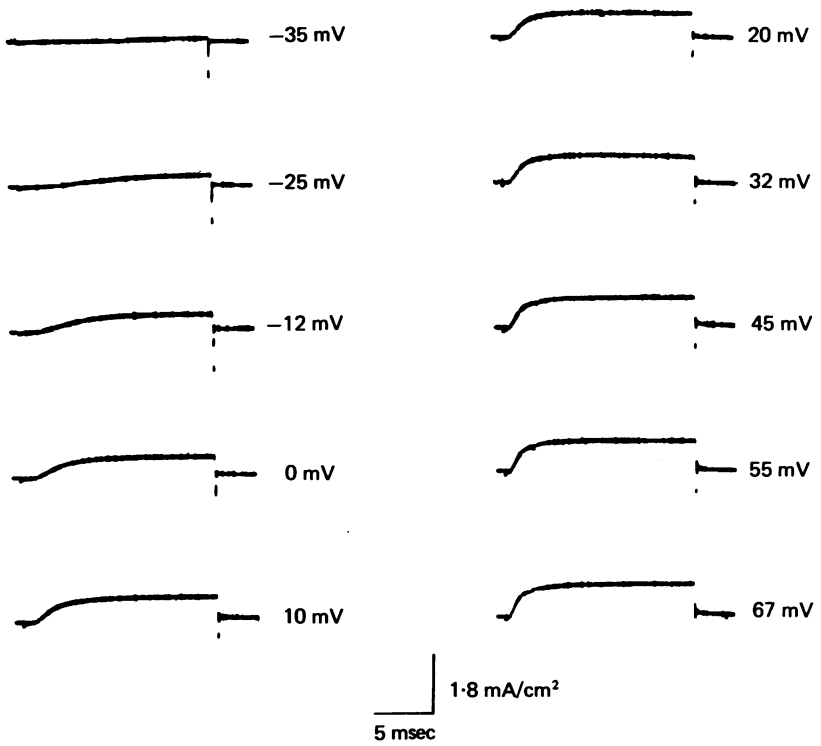

Fig. 20. Delayed currents in an innervated s.m. fibre in the presence of 1 μM-TTX. Fibre depolarized to the potentials shown following a 100 msec conditioning pulse to −143 mV. 23·5 °C. Fibre 8/17/3. Ends cut in K glutamate+EGTA. Balance B–C method.

The time course of currents, $I_K(t)$, can be fitted with conventional n^4 kinetics (Fig. 21) if one allows that potential changes affect the currents only after a delay, Δt:

$$I_K(t+\Delta t) = I_K(\infty)(1-e^{-t/\tau_n})^4, \quad (12)$$

where $I_K(\infty)$ is the peak outward current and τ_n the potential-dependent time constant of the hypothetical first-order variable, n (Adrian *et al.* 1970). The currents could also be fitted without a delay if the exponent in eqn. (12) was doubled; this did not affect the best value of τ_n appreciably. The delay, Δt, in eqn. (12) averaged 0·48 msec at −25 mV and 0·1 msec at 50 mV (four fibres at 20 °C). Fig. 21 (top) shows the voltage dependence of τ_n in three innervated s.m. fibres. The curves are

given by

$$\tau_n = 1/(\alpha_n+\beta_n), \tag{13}$$

$$\alpha_n = \frac{\bar{\alpha}_n (V-\bar{V}_n)}{1-\exp (\bar{V}_n-V)/k_{\alpha n}}, \tag{14}$$

$$\beta_n = \bar{\beta}_n \exp (\bar{V}_n-V)/k_{\beta n} \tag{15}$$

with the parameters $\bar{\alpha}_n$, $\bar{V}_n$, $k_{\alpha n}$, $\bar{\beta}_n$, $k_{\beta n}$ as given in Table 7. In one fibre, τ_n was

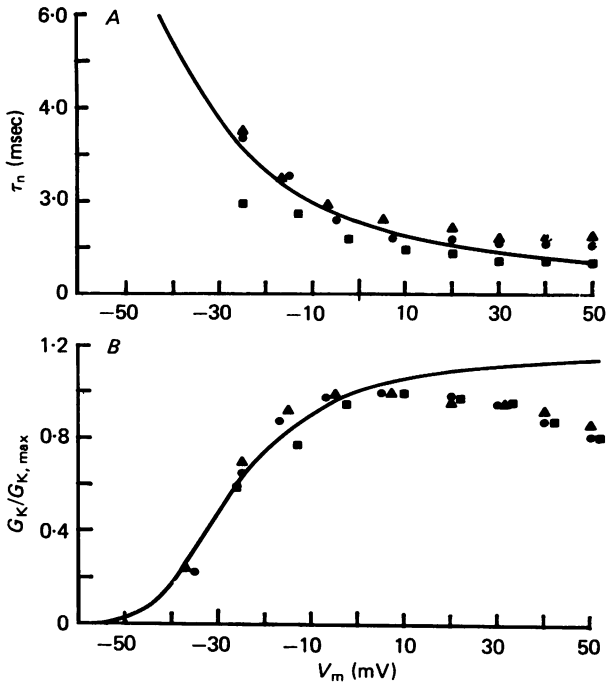

Fig. 21. Time constants and steady-state values of delayed current activation in three innervated s.m. fibres. Top: time constants, τ_n, as a function of voltage. Points calculated from fit of current records with eqn. (12). Curve calculated from eqn. (13) with parameters listed in Table 7. Bottom: relative peak potassium conductance, $G_K/G_{K,max}$, as a function of voltage. Points calculated from same current records as above using eqn. (16). Curve calculated from eqn. (17) with parameters listed in Table 7, normalized to a value of 1 at +5 mV. (■) Fibre 8/17/3, 23·5 °C; (▲) fibre 11/2/2, 21 °C; (●) fibre 11/2/1, 20 °C. Ends cut in K glutamate +EGTA. Balance B–C method.

measured at 10·5 °C and 23·5 °C; the Q_{10} was about 2·5 over the voltage range −40 to +40 mV. Eqns (13)–(15) were developed for frog muscle (Adrian *et al.* 1970) and fit the rat data over the potential range spanned by an action potential. At extreme positive potentials, the measured τ_n seems to reach a limiting value, contrary to what eqn. (13) would predict.

Fig. 21 (bottom) shows, as a function of potential, the normalized peak conductance calculated from

$$G_K = I_K(\infty)/(V_m-V_K), \tag{16}$$

where $V_K = -90{\cdot}5$ mV is the K^+ equilibrium potential calculated from the K^+

concentrations in the C, E pools and in the A pool. In Fig. 21 (bottom), K^+ conductance reached a maximum at about 5 mV and became smaller at more positive potentials. Since measurements were taken in the order of increasing depolarization, the smaller conductance at positive potentials probably is an artifact resulting from

TABLE 7. Parameters for kinetic model of potassium currents

$\bar{\alpha}_n$	0·0132 msec^{-1}
$\bar{\beta}_n$	0·0556 msec^{-1}
$\bar{V}_n$	−40 mV
$k_{\alpha,n}$	7 mV
$k_{\beta,n}$	40 mV

Parameters are from Adrian *et al.* (1970) for frog muscle at 1–3 °C with rate constants scaled by a factor of 3·01, equivalent to a Q_{10} of 2·01 between 2 and 20 °C.

rundown or cumulative inactivation. Inactivation of delayed currents occurs in rat (Duval & Leóty, 1978) and frog skeletal muscle (Adrian *et al.* 1970), and even the 15 sec rest at −90 mV sometimes allowed in Fig. 20 (top) before a depolarization may not have been sufficient for complete recovery from inactivation during preceding depolarizations. The curve is calculated from

$$G_K/G_{K,max} = n_\infty^4 = [\alpha_n/(\alpha_n+\beta_n)]^4, \quad (17)$$

where α_n and β_n are given by eqns (14) and (15). The mean maximal conductance ± S.E. of mean was 11·7 ± 1·8 m-mho/cm^2 in a group of four fibres which includes the three fibres in Fig. 21. This would correspond to a maximal conductance of 7·5 m-mho/cm^2 in uncontracted fibres. The membrane conductance in intact fibres with all channels open may be somewhat larger. First, my measurements may have been contaminated by inactivation, and secondly, an apparently irreversible decline (rundown) of the conductance usually occurred during the course of an experiment. In fact, many fibres showed no delayed outward currents at all, and on the whole, delayed currents gave the impression of being rather labile under the conditions of Fig. 21. The value of 11·7 m-mho/cm^2 should thus be regarded as a lower limit, at least for intact fibres. Even so, it is comparable to that obtained on frog muscle if one corrects for temperature differences. In one fibre with G_K = 9·66 m-mho/cm^2 at 23·5 °C, cooling to 10·5 °C reduced G_K to 6·14 m-mho/cm^2. Calculating from these data a Q_{10} of 1·4, one expects from the fibres in Fig. 21 an average conductance of 8·4 m-mho/cm^2 at 1 °C and 9·9 m-mho/cm^2 at 6 °C. These values are within the range observed on frog muscle by Almers (1976; 2–10 m-mho/cm^2 at 5 °C) and Kovacs & Schneider (1978; 2·1 m-mho/cm^2 for a fibre of 7 μF/cm^2 membrane capacity at 3–4 °C).

DISCUSSION

This paper describes the results of voltage-clamp experiments in normal and denervated fast rat skeletal muscle using the vaseline-gap technique developed by Hille & Campbell (1976) for frog skeletal muscle fibres. This method has the advantage over micro-electrode clamps that good voltage control is possible even for currents as fast and large as the transient sodium current. In addition, external

solutions can be changed easily and rapidly. Since the method uses cut pieces of muscle fibres, the composition of the fibre interior can be manipulated by allowing solutions to diffuse through the cut ends of the fibre. This has the advantages of allowing tests on the effects of substances on the interior of the fibre and the block of contraction in isotonic solution. A disadvantage is that the internal milieu is not normal, and the internal solutions may have unanticipated effects on the membrane properties.

Ionic currents of innervated muscle. This paper presents a kinetic analysis of the sodium and potassium currents of normal rat skeletal muscle. Since the sodium and potassium currents of rat and frog skeletal muscle fibres are so similar, kinetic models developed for frog muscle (Adrian *et al.* 1970; Campbell & Hille, 1976) also apply to the rat with only minor modification. As has been previously observed with micro-electrodes (Adrian & Marshall, 1977), activation of the sodium current occurs at more negative potentials in rat muscle than frog.

Rates of activation of sodium current were comparable to those in frog muscle at positive potentials, but at potentials negative to -40 mV were significantly slower. Adrian & Marshall (1976) calculated that a decrease in activation rate would tend to make the membrane less stable at potentials near rest. In normal muscle, this tendency for instability is countered by the high resting chloride conductance (Palade & Barchi, 1977; Camerino & Bryant, 1976). In myotonic goat muscle, lack of this high chloride conductance (Bryant & Morales-Aguiler, 1971) is thought to give rise to repetitive firing in response to a single stimulus (Adrian & Bryant, 1974).

The rate of inactivation during depolarizing voltage steps were the same as in frog muscle when both were measured at 12 °C. They are similar to those found by Duval & Leóty (1978) in intact fibres at 15–17 °C, but are faster than reported by Adrian & Marshall (1977) at 14 °C. The reason for the discrepancy is not clear. Recovery from inactivation was much slower than in frog with an average time constant of 40 msec at -100 mV and 12 °C.

The voltage dependence of inactivation was highly variable in these experiments and was often shifted to more negative potentials than expected from results in intact fibres. Shifted h_∞ curves occurred at both 12 and 20 °C, in contrast to results in sheep Purkinje fibres where negative h_∞ curves measured at low temperatures shifted to more positive potentials upon warming to 20 °C (Dudel & Rüdel, 1970). The most positive h_∞ relations were similar to those measured in intact rat muscle (Adrian & Marshall, 1977; Duval & Leoty, 1978). Since the inactivation mechanism seems to be relatively accessible to modification from the inside in other excitable cells, the more negative h_∞ curves found in these experiments may result from the abnormal internal composition of the cut fibres. Indeed, there is some indication in the present experiments that the inactivation process is different in cut fibres. A careful comparison of the properties of cut and intact fibres may provide useful information on the effects of the interior environment on channel functions.

The peak sodium conductance in innervated e.d.l. fibres averaged 40–50 m-mho/cm^2 at 12 °C correcting for fibre contraction. The density of binding sites for saxitoxin in innervated e.d.l. fibres is $535 \pm 43/\mu m^2$ (Hansen Bay & Strichartz, 1980). If, as in frog nerve, only half the sodium channels are open at the time of the peak current (Sigworth, 1978), a single channel conductance of 1·68 p-mho can be calculated from

these data. The single channel conductance calculated here is in the same range as estimates for frog muscle (Almers & Levinson, 1975), and nerve (Conti, Hille, Neumcke, Nonner and Stämpfli, 1976) which range from 1 to 8 p-mho.

Potassium currents were similar in magnitude and voltage dependence to those of frog muscle. When scaled by the experimentally determined Q_{10} of 2·5, activation rates are also comparable to measurements in frog at 2 °C (Adrian *et al.* 1970).

The kinetic analysis presented here in conjunction with the temperature coefficients measured can be used to calculate action potentials in mammalian muscle under physiological conditions. This should provide a more accurate estimate of the normal electrical behaviour than previous calculations, which relied on data from frog muscle at 4 °C in hypertonic solutions (Adrian & Marshall, 1976).

Sodium currents in denervated muscle. Activation and inactivation were shifted by ~10 mV to more negative potentials following denervation. Rates of activation and inactivation were not measurably different from innervated fibres, although there was enough scatter that a 10 mV shift might not be discerned. Since the resting potential of denervated rat muscle is depolarized relative to normal (Albuquerque & McIssac, 1970; Redfern & Thesleff, 1971*a*), the shift in activation could lead to significant sodium current at the resting potential. Anode break action potentials are present in denervated, but not innervated, rat muscle, even when both are depolarized to the same level following anode break (Marshall & Ward, 1974) and application of TTX increases the resting potential of denervated, but not innervated, muscle (Harris & Thesleff, 1971). Both phenomena can be explained by a sodium conductance activated at rest potential. The shifted activation may also explain the spontaneous oscillations in membrane potential which can cause fibrillation in denervated mammalian muscle (Purves & Sakmann, 1974). These oscillations are sodium-dependent and are blocked by 5 μM-TTX, indicating that sodium currents are involved in their initiation.

The maximum peak sodium conductance in denervated muscle is similar, within a factor of two, to that in innervated fibres, consistent with the similar saxitoxin binding capacities of e.d.l. and diaphragm before and after denervation (Ritchie & Rogart, 1977; Hansen Bay & Strichartz, 1980). These results are somewhat puzzling in light of the observation that the $\bar{V}_{max}$ of the action potential is two-thirds the normal in denervated muscle (Albuquerque & Thesleff, 1968; Alburquerque & McIssac, 1970; Redfern & Thesleff, 1971*a*). The reduction in $\bar{V}_{max}$ could be due to inactivation of the sodium current in denervated muscle, which would be reversed in the present experiments by the negative holding potential (−90 mV) employed. If such a process were involved, the rate constants for recovery would have to be very slow, since conditioning hyperpolarizations lasting 30–60 sec are insufficient to restore $\bar{V}_{max}$ to normal levels (Redfern & Thesleff, 1971*a*). The apparent shift in h_∞ could, if present in intact fibres, contribute to the reduction in $\bar{V}_{max}$.

Effects of tetrodoxin. In innervated rat muscle, TTX blocks sodium channels without affecting the kinetics of the unblocked channels. The dose–response relation is well described by assuming a single class of receptors for TTX with a K_d = 5 nM. This value is comparable to that obtained from binding studies in rat diaphragm (Colquhoun, Rang & Ritchie, 1974) and frog muscle (Almers & Levinson, 1975).

In denervated rat muscle, sodium currents remain in 1 μM TTX. These TTX-

resistant currents differ in their kinetics from the sodium currents in normal Ringer solution. The slower kinetics cannot be explained by a preferential location of the resistant currents in the tubular membrane for the reasons discussed in the Results. This has also been concluded from studies of the TTX-resistant action potential in glycerol-treated denervated rat diaphragm (Colquohoun *et al.* 1974). From the present conductance measurements and the results of binding studies (Ritchie & Rogart, 1977), it seems that the normal population of sodium channels is retained following denervation. The simplest explanation of these results is that denervation induces the appearance of a new population of sodium channels. This interpretation is consistent with the dose-response relation for TTX, which could be fitted well assuming the presence of a second population of channels with a K_D of 1 μM in addition to the normal channels.

It is a pleasure to thank Dr Wolfhard Almers for his generous support, advice and helpful suggestions throughout the course of this work. I am grateful to Dr Bertil Hille for the use of equipment and chemicals and for stimulating discussion.

I was supported by a National Research Service Award from the National Institute of Health (GMO7270). The research expenses for this study were defrayed by USPHS grant no. AM17803.

REFERENCES

ADRIAN, R. H. & ALMERS, W. (1974). Membrane capacity measurements of frog skeletal muscle in media of low ion content. *J. Physiol.* **237**, 573–605.

ADRIAN, R. H. & BRYANT, S. H. (1974). On the repetitive discharge in myotonic muscle fibres. *J. Physiol.* **240**, 505–515.

ADRIAN, R. H., CHANDLER, W. K. & HODGKIN, A. L. (1969). The kinetics of mechanical activation in frog muscle. *J. Physiol.* **204**, 207–230.

ADRIAN, R. H., CHANDLER, W. K. & HODGKIN, A. L. (1970). Voltage clamp experiments in striated muscle fibres. *J. Physiol.* **208**, 607–644.

ADRIAN, R. H. & MARSHALL, M. W. (1976). Action potentials reconstructed in normal and myotonic muscle fibres. *J. Physiol.* **285**, 125–143.

ADRIAN, R. H. & MARSHALL, M. W. (1977). Sodium currents in mammalian muscle. *J. Physiol.* **268**, 223–250.

ADRIAN, R. H. & PEACHEY, L. D. (1973). Reconstruction of the action potential of frog sartorius muscle. *J. Physiol.* **235**, 103–131.

ALBUQUERQUE, E. X. & MCISSAC, R. J. (1970). Fast and slow mammalian muscles after denervation. *Expl Neurol.* **26**, 183–202.

ALBUQUERQUE, E. X. & THESLEFF, S. (1968). A comparative study of membrane properties of innervated and chronically denervated fast and slow skeletal muscles of the rat. *Acta physiol. scand.* **73**, 471–480.

ALMERS, W. (1976). Differential effects of tetracaine on delayed potassium channels and displacement currents in frog skeletal muscle. *J. Physiol.* **262**, 613–637.

ALMERS, W. & LEVINSON, S. R. (1975). Tetrodotoxin binding to normal depolarized frog muscle and the conductance of a single sodium channel. *J. Physiol.* **247**, 483–509.

ARMSTRONG, C. M. & HILLE, B. (1972). The internal quaternary ammonium ion receptor in potassium channels of the node of Ranvier. *J. gen. Physiol.* **59**, 388–400.

BASTIAN, J. & NAKAJIMA, S. (1974). Action potential in the transverse tubules and its role in the activation of skeletal muscle. *J. gen. Physiol.* **63**, 257–278.

BRYANT, S. H. & MORALES-AGUILER, A. (1971). Chloride conductance in normal and myotonic muscle fibres and the action of monocarboxylic aromatic acids. *J. Physiol.* **219**, 367–383.

CAMERINO, D. & BRYANT, S. H. (1976). Effects of denervation and colchicine treatment on the chloride conductance of rat skeletal muscle fibres. *J. Neurobiol.* **7**, 221–228.

CAMPBELL, D. T. (1976). Ionic selectivity of the sodium channel of frog skeletal muscle. *J. gen. Physiol.* **67**, 295–307.

CAMPBELL, D. T. & HILLE, B. (1976). Kinetic and pharmacological properties of the sodium channel of frog skeletal muscle. *J. gen. Physiol.* **67**, 309–323.

CHIU, S. Y. (1977). Inactivation of sodium channels: second order kinetics in myelinated nerve. *J. Physiol.* **273**, 573–596.

COLQUHOUN, D., RANG, H. P. & RITCHIE, J. M. (1974). The binding of tetrodotoxin and α-bungarotoxin to normal and denervated mammalian muscle. *J. Physiol.* **240**, 199–226.

CONTI, F., HILLE, B., NEUMCKE, B., NONNER, W. & STÄMPFLI, R. (1976). Measurement of the conductance of the sodium channel from current fluctuations at the node of Ranvier. *J. Physiol.* **262**, 699–727.

COSTANTIN, L. L. (1970). The role of sodium current in the radial spread of contraction in frog muscle fibres. *J. gen. Physiol.* **55**, 703–715.

CREESE, R., EL-SHAFIE, A. L. & VRBOVÁ, GERTA (1968). Sodium movements in denervated muscle and the effects of antimycin A. *J. Physiol.* **197**, 279–294.

DODGE, F. A. & FRANKENHAEUSER, B. (1958). Membrane currents in isolated frog nerve fibre under voltage clamp conditions. *J. Physiol.* **143**, 76–90.

DUDEL, J. & RÜDEL, R. (1970). Voltage and time dependence of excitory sodium current in cooled sheep Purkinje fibres. *Pflügers Arch.* **315**, 136–158.

DULHUNTY, ANGELA, F. & FRANZINI-ARMSTRONG, CLARA (1977). The passive electrical properties of frog skeletal muscle fibres at different sarcomere lengths. *J. Physiol.* **266**, 687–711.

DUVAL, A. & LEÓTY, C. (1978). Ionic currents in mammalian fast skeletal muscle. *J. Physiol.* **278**, 403–423.

EISENBERG, B. R. & KUDA, A. M. (1975). Sterological analysis of mammalian skeletal muscle. II. White vastus muscle of the adult guinea pig. *J. Ultrastruc. Res.* **51**, 176–187.

FALK, G. & FATT, P. (1964). Linear electrical properties of striated muscle fibres observed with intracellular electrodes. *Proc. R. Soc.* B **160**, 69–123.

FINK, R. & WELTWER, E. (1978). Modified K-channel gating by exhaustion and the block by internally applied TEA^+ and 4-aminopyridine in muscle. *Pflügers Arch.* **374**, 289–292.

FRANKENHAUSER, B. (1957). A method for recording resting and action potentials in the isolated frog myelinated nerve fibre. *J. Physiol.* **136**, 550–559.

GOLDMAN, D. E. (1943). Potential, impedance, and rectification in membranes. *J. gen. Physiol.* **27**, 37–60.

GRAMPP, W., HARRIS, J. B. & THESLEFF, S. (1972). Inhibition of denervation changes in skeletal muscle by blockers of protein synthesis. *J. Physiol.* **221**, 743–754.

HANSEN BAY, CHRISTINA & G. R. STRICHARTZ (1980). Saxitoxin binding to sodium channels of rat skeletal muscle. *J. Physiol.* **300**, 89–103.

HARRIS, J. B. & THESLEFF, S. (1971). Studies on tetrodotoxin resistant action potentials in denervated skeletal muscle. *Acta physiol. scand.* **83**, 382–388.

HILLE, B. (1968). Pharmacologic modifications of the sodium channels of frog nerve. *J. gen. Physiol.* **51**, 199–219.

HILLE, B. (1971). The permeability of the sodium channel to organic cations in myelinated nerve. *J. gen. Physiol.* **58**, 599–619.

HILLE, B. (1972). The permeability of the sodium channel to metal cations in myelinated nerve. *J. gen. Physiol.* **59**, 637–658.

HILLE, B. & CAMPBELL, D. T. (1976). An improved vaseline gap voltage clamp for skeletal muscle fibres. *J. gen. Physiol.* **67**, 265–293.

HODGKIN, A. L. & HUXLEY, A. F. (1952). A quantitative description of the membrane current and its application to conduction and excitation in nerve. *J. Physiol.* **117**, 500–544.

HODGKIN, A. L. & KATZ, B. (1949). The effect of sodium ions on the electrical activity of giant axons of squid. *J. Physiol.* **108**, 37–77.

HODGKIN, A. L. & NAKAJIMA, S. (1972). The effects of fibre diameter on the electrical constants of frog skeletal muscle fibres. *J. Physiol.* **221**, 105–120.

IDELFONSE, M. & ROY, G. (1972). Kinetic properties of the sodium current in striated muscle fibres on the basis of the Hodgkin-Huxley theory. *J. Physiol.* **227**, 419–431.

KIYOHARA, T. & SATO, M. (1967). Membrane constants of red and white muscle fibres in the rat. *Jap. J. Physiol.* **17**, 720–725.

KOVACS, L. & SCHNEIDER, M. F. (1978). Contractile activation by voltage clamp depolarization of cut skeletal muscle fibres. *J. Physiol.* **227**, 483–506.

LUFF, A. R. & ATWOOD, H. L. (1971). Changes in the sarcoplasmic reticulum and transverse

tubular system of fast and slow skeletal muscles of the mouse during postnatal development. *J. cell. Biol.* **51**, 369–383.

MANDRINO, MONIQUE (1977). Voltage-clamp experiments on frog single skeletal muscle fibres: evidence for a tubular sodium current. *J. Physiol.* **269**, 605–625.

MARSHALL, M. W. & WARD, M. R. (1974). Anode break excitation in denervated rat skeletal muscle fibres. *J. Physiol.* **236**, 413–420.

NONNER, W. (1978). Zur Inaktrivierung der Natrium poren erregbarer Membranen: Beziehung zur Bewegung geladner Strukturen in der Schnurringsmembran. Habilitationsschrift:Universität des Saarlandes.

PALADE, P. T. & BARCHI, R. L. (1977). Characteristics of the chloride conductance in muscle fibres of the rat diaphragm. *J. gen. Physiol.* **69**, 325–342.

PAPPONE, P. (1977). Voltage clamp experiments on normal and denervated rat skeletal muscle fibres. *Biophys. J.* **17**, 3a.

PURVES, D. & SAKMANN, B. (1974). Membrane properties underlying spontaneous activity of denervated muscle fibres. *J. Physiol.* **239**, 125–153.

REDFERN, P. & THESLEFF, S. (1971*a*). Action potential generation in denervated rat skeletal muscle. I. Quantitative aspects. *Acta physiol. scand.* **81**, 557–564.

REDFERN, P. & THESLEFF, S. (1971*b*). Action potential generation in denervated rat skeletal muscle. II. The action of tetrodotoxin. *Acta physiol. scand.* **82**, 70–78.

RITCHIE, J. M. & ROGART, R. B. (1977). The binding of labelled saxitoxin to the sodium channels in normal and denervated mammalian muscle, and in amphibian muscle. *J. Physiol.* **269**, 341–354.

ROBBINS, N. (1977). Cation movements in normal and short-term denervated rat fast-twitch muscle. *J. Physiol.* **271**, 605–624.

ROBINSON, R. A., & STOKES, R. H. (1965). *Electrolyte Solutions*. London: Butterworth.

SCHWARTZ, W., PALADE, P. T. & HILLE, B. (1977). Local anesthetics: effect of pH on use-dependent block of sodium channels in frog muscle. *Biophys. J.* **20**, 343–368.

SIGWORTH, F. J. (1978). Fraction of sodium channels open at peak conductance. *Biophys. J.* **21**, 41a.

VALDIOSERA, R., CLAUSEN, C. & EISENBERG, R. S. (1974). Impedance of frog skeletal muscle fibres in various solutions. *J. gen. Physiol.* **63**, 460–491.

ZOLOVICK, A. J., NORMAN, R. L. & FEDDE, M. R. (1970). Membrane constants of muscle fibres of rat diaphragm. *Am. J. Physiol.* **219**, 654–757.